SOVIET PHYSICS

USPEKHI

A Translation of Uspekhi Fizicheskikh Nauk

SOVIET PHYSICS USPEKHI (Russian Vol. 94, Nos. 3 and 4) SEPTEMBER-OCTOBER 1968

535.4

EMISSION FROM CHARGED PARTICLES IN PERIODIC STRUCTURES

B. M. BOLOTOVSKIĬ and G. V. VOSKRESENSKIĬ

P. N. Lebedev Institute of Physics, USSR Academy of Sciences;
Radiotechnical Institute, USSR Academy of Sciences

Usp. Fiz. Nauk 94, 377—416 (March, 1968)

INTRODUCTION

As we know, motion of charged particles in an optically inhomogeneous medium is accompanied by emission of electromagnetic waves. A typical example is transition radiation, which arises when a charged particle in uniform motion passes through the boundary between two homogeneous media having different optical properties.[1] Another example is diffraction emission, which appears when electromagnetic-field sources pass close to ideally-conductive bodies.[2,3]. The emission from a charged particle passing alongside periodically-repeated inhomogeneities shows a number of specific physical characteristics. This article is devoted to discussing this particular case. Study of emission from charged particles in periodic structures is of interest in connection with a number of possible physical applications. One of them is generation of electromagnetic radiation by a beam of charged particles interacting with a periodic structure. Another possible application is to determine the characteristics of the emitting particle (velocity, charge, and trajectory) from the properties of the field that it emits. Study of the interaction of charged particles with periodic structures is also of interest because the design of many instruments in modern electronics (e.g., linear accelerators) is based on it. The cited reasons explain at least partly the fact that many experimental and theoretical studies have appeared in recent years on the interaction of charged particles with periodically inhomogeneous media. The published studies have discussed mainly two sets of problems: the possibility of generating radiation in a given region of the optical range by interaction of charged particles with a periodic system (a diffraction grating), and the possibility of detecting relativistic charged particles by the emission from them in a periodic medium. Both of these possibilities have already been realized experimentally. While we must consider the obtained results as being preliminary in many ways, it is à propos to discuss the status of the theory and experiment in this field in order to envision the possible directions of development more clearly.

The first part of this review will discuss emission from charged particles moving in the vicinity of a diffraction grating. Here we shall pay attention not to studying concrete models, but rather to elucidating the general characteristics of emission in periodic structures.

The second section will deal mainly with discussing models that permit an exact solution of the problem. While one must sometimes have recourse to a highly idealized model to obtain an exact solution, nevertheless the obtained results are of some practical value in permitting one to make quantitative estimates.

The discussion deals with open structures. In distinction from closed resonators, the radiation field in these can propagate freely to arbitrarily large distances from the trajectory of the source.

I. EMISSION FROM A SOURCE PASSING OVER A PLANE DIFFRACTION GRATING

Insofar as we know, I. M. Frank[4] was the first to indicate in 1942 that electromagnetic waves could be emitted by a source moving near a diffraction grating. E. Purcell independently came to analogous conclusions; he and S. Smith were the first to detect such an emission, and they performed the first experimental studies.[5]

In the experiments of Smith and Purcell, a well-focused beam of electrons of energy of the order of 300 keV passed over a flat optical reflective diffraction grating of period $d = 1.67\ \mu$. The beam lay parallel to the plane of the grating and perpendicular to the ruling;

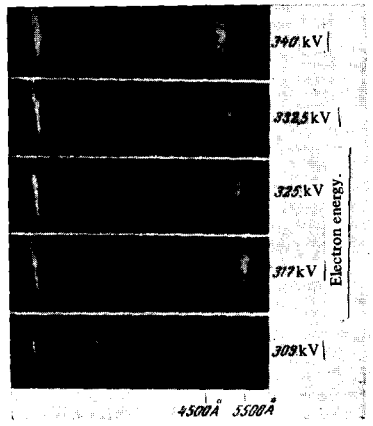

FIG. 1.

the distance of the beam from the plane of the grating was made as small as possible. As the authors note, the electron beam almost touched the grating.

Under these conditions, radiation appeared that was visible to the naked eye. The region where the beam passed over the grating had the appearance of a sharp glowing colored line on the surface of the grating when observed at an angle of 20–30° to the travel of the beam. Here the "color" of the visible radiation varied with varying electron velocity or angle of observation.

In order to analyze the spectral composition of the radiation emitted at a given angle, they used a transparent diffraction grating. The radiation traveling at the given angle was isolated with a special collimating apparatus. After passing through an analyzing grating, the radiation entered the objective of a camera focused at infinity, and was recorded on film. Figure 1 gives the spectrograms from [5] for the emission angle $\theta = 20°$. The bright vertical line at the left, which occurs on all the spectrograms, corresponds to rays normally incident on the analyzing grating and passing through it without deviation. The bright line at the right corresponds to the first-order diffraction peak. The wavelength of the radiation for the first peak is indicated on the spectrogram. The figure shows several spectrograms for different electron energies in the beam. We see that the wavelength of the emission decreases with increasing energy. The intensity of the emission was not measured in [5].

We can analyze the results of Purcell and Smith's experiment in terms of simple qualitative considerations. Let us imagine a charged particle in uniform motion close to a flat diffraction grating (Fig. 2). As will be shown, the emission spectrum is determined only by the period of the grating, and does not depend on other features of it (e.g., the profile of the grating, or whether it is transparent or reflective). Hence, we shall carry out the treatment for a flat, transparent grating of period d. Let a plane wave of radiation $\exp\{i\mathbf{k}\cdot\mathbf{r} - i\omega t\}$ be produced as the charge passes by one of the lines of the grating. Here k is the wave vector, which lies at the angle θ to the velocity of the charge. Then, when the charge passes by the next line of the grating, the wave $\exp\{i\mathbf{k}\cdot(\mathbf{r} - \mathbf{d}) - i\omega(t - \Delta t)\}$ is emitted. Here $\Delta t = d/u$ is the time of flight of the charge through one period of the structure. Evidently the emission from adjacent lines of the grating will not be ex-

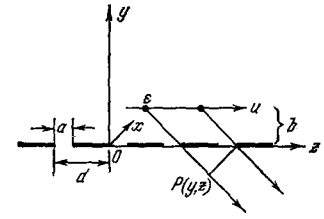

FIG. 2.

tinguished if the phase difference of the corresponding waves is a multiple of 2π:

$$\omega\Delta t - \mathbf{kd} = \omega\frac{d}{u} - kd\cos\theta = \frac{\omega d}{u}(1 - \beta\cos\theta) = 2\pi n. \qquad (1)$$

where we have used the relation $k = \omega/c$. Of course, this treatment is valid for a reflecting diffraction grating, as well as for any other periodic structure. As Eq. (1) implies, waves of different frequencies are emitted at a given angle of observation θ:

$$\omega_n = \frac{2\pi n\frac{u}{d}}{1 - \beta\cos\theta}. \qquad (2)$$

Equations (1) and (2) give the relation of the emission frequency to the velocity of the source, the angle of observation, and the period of the structure. The emission spectrograms obtained by Smith and Purcell quantitatively verify these formulas. In fact, if we assume, as was the case in the experiment, that $d = 1.67 \times 10^{-4}$ cm, $\theta = 20°$, and $\beta = 0.8$ (corresponding to an electron energy of 300 keV), we get from Eq. (2) for $n = 1$ (the fundamental emission frequency) a wavelength of radiation close to 5000 Å (see Fig. 1). The authors also observed frequencies that were multiples of the fundamental, corresponding to values of n from one to five.

Almost ten years after Purcell and Smith's experiments, statements have appeared that a generator of electromagnetic radiation based on the same principle has been built. [6] This instrument was developed in the laboratories of the Varo company, and was called the varotron. The radiation source in it was electrons passing close to a flat optical diffraction grating. The varotron permitted easy variation of the emitted frequency over the wavelength range from 10^{-4} to 0.5×10^{-4} cm, i.e., in the infrared to the limits of the visible. Along with the fundamental, the varotron also emitted higher harmonics up to the ultraviolet. Human speech has been transmitted with the varotron, both with frequency and amplitude modulation.

Recently a description of another device has appeared. It is based on interaction of an electron beam with a periodic diffraction structure. [7] A diagram of the device, which the authors called the orotron (a device with an open resonator and a reflecting grating), is shown in Fig. 3. The open resonator is formed by a flat and a spherical mirror whose distance can be varied continuously. Teeth were cut in the surface of the flat mirror. The power generated in the resonator emerged through an aperture in the spherical mirror. A flat electron beam was generated by a diode gun, was shaped by a diaphragm, and accelerated by a d.c. or pulsed voltage. The beam was focused by a strong longitudinal magnetic field. Generation of waves in the millimeter range was observed in the device. Here the frequency

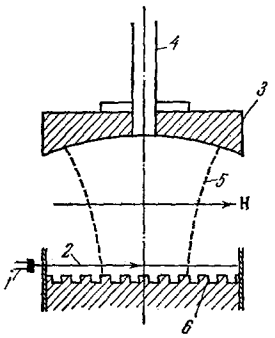

FIG. 3. Diagram of the orotron. 1 – electron gun; 2 – electron beam; 3 – spherical mirror; 4 – waveguide; 5 – caustic limiting the field; 6 – toothed retarding structure.

depended on the distance between the mirrors and on the accelerating voltage. The output power depended practically linearly on the beam current. The pulsed output power was quite considerable. Thus, for a current ~ 1 A, the pulsed output power at a wavelength of 8.1 mm amounted to about 4 watts.

The described device is an autogenerator of ultrahigh-frequency oscillations using an electron beam. The feedback that can be realized with an open resonator permits one to transform the incoherent radiation of the electron beam passing over a periodic structure into coherent monochromatic radiation.

A Qualitative Treatment of the Features of the Emission

Equations (1) and (2), which give the spectrum of the radiation produced when a charge moves in the vicinity of a periodic structure, can be derived from the laws of conservation of energy and momentum. In addition to them, we use only the fact that the structure is periodic.

Let us consider the features of a field in a linear periodic structure. As we know from the theory of equations having periodic coefficients, the field component corresponding to a given frequency ω can be represented in a periodic structure as a superposition of fields:

$$\mathbf{E}_\omega(\mathbf{r}) = \mathbf{A}(\mathbf{r})\, e^{i\varkappa(\omega) z}, \tag{3}$$

Here $\varkappa(\omega)$ is defined by solving the boundary problem in electrodynamics, and $\mathbf{A}(\mathbf{r})$ is a periodic function of the variable z having the period d of the structure (we assume that the system being treated is periodic along the z axis). If we expand $\mathbf{A}(\mathbf{r})$ in a Fourier series in the variable z, we get

$$\mathbf{E}_\omega(\mathbf{r}) = \sum_{n=-\infty}^{\infty} \mathbf{A}_n(x, y)\, e^{i\left[\varkappa(\omega) + \frac{2\pi n}{d}\right] z}. \tag{4}$$

As we see from Eq. (4), the field for a given frequency ω is a sum of waves. The values of their longitudinal components of the wave vector,

$$k_z = \varkappa(\omega) + \frac{2\pi}{d} n \tag{5}$$

differ by a quantity which is a multiple of

$$k_0 = \frac{2\pi}{d}. \tag{6}$$

Considering the well-known quantum-mechanical relation between the momentum and the wave vector:

$$\mathbf{p} = \hbar\mathbf{k}, \tag{7}$$

we can state that the longitudinal component of the momentum of a photon in a linear periodic medium can vary only by an amount which is a multiple of the elementary momentum

$$\mathbf{p}_0 = \hbar k_0 \mathbf{z}_0 = \frac{2\pi\hbar}{d}\, \mathbf{z}_0, \tag{8}$$

Here $\mathbf{z}_0$ is a unit vector lying along the axis of periodicity of the system. This is equivalent to stating that a linear periodic system can acquire an integral multiple of the elementary momentum $\mathbf{p}_0$.

Now we shall let the charge moving in the periodic system emit a quantum of light of momentum $\hbar\mathbf{k}$ and energy $\hbar\omega$. We shall write down the laws of conservation of energy and momentum. If we denote the energy E and momentum p of the charge before emission with the subscript 1, and after emission by the subscript 2, we get

$$\begin{aligned} \mathbf{p}_1 - \mathbf{p}_2 &= \Delta\mathbf{p} = \hbar\mathbf{k} + n\hbar\mathbf{k}_0, \\ E_1 - E_2 &= \Delta E = \hbar\omega. \end{aligned} \tag{9}$$

Let us form the scalar product of the first equation by the velocity $\mathbf{u}$ of the charge. Using the relation $\mathbf{u} \cdot \Delta\mathbf{p} = \Delta E$, which holds for small variations in the energy of the particle, we get

$$\mathbf{u} \cdot \Delta\mathbf{p} = \Delta E = \hbar\omega = \hbar\mathbf{k} \cdot \mathbf{u} + n\hbar\mathbf{k}_0 \cdot \mathbf{u}. \tag{10}$$

Hence, taking into account the relation $k = \omega/c$, we get

$$\omega = n(\mathbf{k}_0 \cdot \mathbf{u})/[1 - (u/c)\cos\theta], \tag{11}$$

where θ is the angle between the velocity of the charge and the direction of emission.

In the special case in which the velocity $\mathbf{u}$ of the particle is parallel to the vector $\mathbf{k}_0$ (or equivalently, the velocity of the particle is parallel to the axis of periodicity of the system), we obtain from (11) the relation (2) given previously. In connection with the derived formulas, we note first of all that the formulas for the emission spectrum prove to be purely classical (they do not contain Planck's constant $\hbar$), in spite of their quantum derivation. The reason for this lies in the above-mentioned assumption that the variation in the energy of the charge in the emission process is small. It is evident from the derivation that the emission spectrum is independent of the concrete form of the system, and is determined by its period alone.

Equation (11) admits of a simple physical interpretation. In fact, the numerator of Eq. (11) contains the quantity $n(\mathbf{k}_0 \cdot \mathbf{u})$, which is an integral multiple of the "frequency of passage" of the charge through one period of the structure. On the other hand, the denominator contains a characteristic Doppler factor accounting for the motion of the particle. Motion of a particle in a periodic structure involves inducing a charge on the surfaces of the structure. The induced charge periodically varies in time with the fundamental period $T = d/u$, which is equal to the time of passage of the particle through one unit of the structure. This periodically-varying induced charge, which moves along with the uniformly-moving charged particle, is the source of the emission.

We see from Eqs. (2) and (11) that several emission waves can exist at the given frequency ω. They differ in the values of the emission angle θ and the order n of the spectral line. The number of emitted waves is determined by the obvious requirement

$$-1 \leqslant \cos\theta_m = \left(\frac{1}{\beta} - \frac{2\pi}{kd}m\right) \leqslant +1, \tag{12}$$

whence

$$\frac{kd}{2\pi}\left(\frac{1}{\beta}+1\right) \geqslant m \geqslant \frac{kd}{2\pi}\left(\frac{1}{\beta}-1\right). \tag{13}$$

The minimum number of emitted lines Δm is determined by the integral part of the quantity

$$\frac{kd}{\pi} = 2\frac{d}{\lambda} \tag{14}$$

(λ is the emission wavelength). We see that the number of harmonics emitted at a given frequency does not depend on the velocity of the source.

If we fix the order m of the spectral line, then Eqs. (11)–(13) imply an inequality determining the frequency band of emission of a charge moving at the fixed velocity $\beta = u/c$:

$$\frac{\beta m}{1-\beta} \geqslant \frac{kd}{2\pi} \geqslant \frac{\beta m}{1+\beta}. \tag{15}$$

We shall return below to the derived relations in discussing concrete models of periodic structures.

The cited general characteristics of the emission spectrum do not depend on the concrete form of the periodic structure. We can also state some general considerations on the intensity of emission, based on the properties of the field of a uniformly-moving charge. Since the field of the charge declines with increasing distance from its trajectory, the amplitude of the induced currents declines with increasing impact parameter b (the distance from the trajectory to the structure). Consequently, the emission intensity also declines. The relation of the spectral components of the field of a uniformly-moving source to the impact parameter has the form

$$E,\ H \sim e^{-k\gamma b}, \tag{16}$$

where

$$k = \frac{\omega}{c},\quad \gamma = \frac{\sqrt{1-\beta^2}}{\beta},\quad \beta = \frac{u}{c}. \tag{17}$$

The reduced currents show the same dependence on the impact parameter. Evidently the intensity of emission is proportional to the square of the factor in (16). As we see, the intensity of emission at a given frequency declines rapidly with increasing impact parameter. Hence the distance of the passing charge from the structure must be as small as possible. We note that the parameter γ declines with increasing energy of the particles, and the permissible value of the impact parameter b increases.

II. PHYSICAL MODELS OF DIFFRACTION GRATINGS AND METHODS OF CALCULATION

The properties of the emission that we have discussed thus far are general for all periodic structures, and do not depend on the concrete model of the structure. The emission spectrum is determined only by the fact that the structure is periodic; the relation of the intensity to the impact parameter stems from the law of decline of the field of a uniformly-moving source. In order to determine the remaining properties of the emission, e.g., the angular or spectral distribution, we must deal with a concrete physical model of the periodic structure.

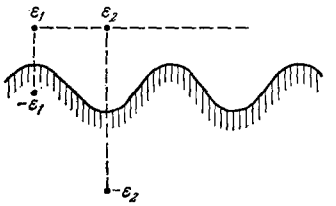

FIG. 4.

The first estimate of the emission intensity was made in the above-discussed study by Smith and Purcell.[5] We shall give here only the gist of their discussions.

Let the reflective diffraction grating be an ideally reflective corrugated surface (Fig. 4). As the charge moves above such a surface, currents are induced in it. If the surface doesn't differ greatly from a plane (i.e., the corrugation is of small depth and long period), and if the charge passes close to the surface, then the induced currents can be reduced to the motion of a point image charge, i.e., a charge of the same magnitude and opposite sign situated symmetrically opposite the source with respect to the grating surface. We see from Fig. 4 that when the source is over a crest of the grating, the distance between the source and its image is smaller than when the source is over a trough. Thus, the moving source and its image form a dipole whose magnitude varies periodically in time. Then we identify the emission from this variable dipole with the emission from the source moving above the grating. This scheme gives the formula (2) derived above for the emission spectrum. We can estimate the emission intensity by using the expression for the energy emitted from an oscillator of moment p at the wavelength λ:[8]

$$\frac{dW}{dt} = \frac{16\pi^4 c}{3\lambda^4}p^2 \tag{18}$$

(Here we have used the formula for the energy emitted from an oscillator at rest, i.e., its motion is thus far neglected). In Eq. (18), p denotes the amplitude of variation of the dipole moment, as determined by the distance from the charge to the grating. Now let the electrons pass close to the grating, so that their distance from the grating is a tenth of the period (this estimate was adopted in[5]). Then $p = \epsilon d/10$, where ϵ is the magnitude of the charge passing above the grating. Substitution of parameters corresponding to the experiments of Smith and Purcell into Eq. (18) gives a value of the order of several hundred for the number of photons emitted per cm of path above the grating. The same number of photons in order of magnitude is emitted in the Cerenkov effect.

The simple model of the diffraction grating adopted by Smith and Purcell for estimating the emission intensity was also used by Ishiguro and Tako.[9] Here they tried to construct a more exact image of the source with respect to a curvilinear ideally-conductive surface, and to estimate the effect of the shape of the reflective grating on the size and orientation of the dipole moment of the effective emission source. As we can see from Fig. 5, the effective dipole has components along both the z and y axes. Let the charge be situated at the point having coordinates (z, s). We can easily see that the line joining the charge with its image intersects the surface of the grating at the point $(z + \xi, y(z + \xi))$,

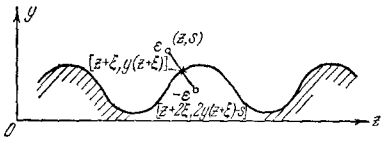

FIG. 5.

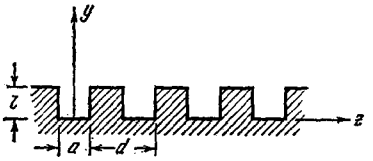

FIG. 6.

where y = y(z) is the equation of the surface of the grating. The quantity ξ is proportional to the component of the dipole along the z axis, and is determined from the equation $\xi = [(s - y)y']_{z+\xi}$. If the grating is smooth enough ($y' \ll 1$), the depth of modulation being much less than the period, then the longitudinal component of the effective dipole, which is proportional to the small quantity ξ, can be neglected in comparison with its vertical component (at least in estimating the total emission intensity).

Thus far, in estimating the emission intensity, we have not taken into account the Doppler shift of the frequency of the effective oscillator formed by the moving charge and its image in the grating. We can do this by using the expression for the angular distribution of the emission from a moving system of charges.[8] If we describe the emission under discussion by the model of a moving oscillator oriented normal to the plane of the diffraction grating, then we get the following for the angular distribution of emission:[10]

$$dI = \frac{p^2 4\pi^3}{c^3}\left(\frac{u}{d}\right)^4 \frac{(\cos\theta-\beta)^2}{(1-\beta\cos\theta)^5}\,d\theta, \tag{19}$$

Here the angle of observation θ is measured from the plane of the grating, and p is the moment of the effective dipole. Let us determine the moment of the effective dipole for a reflective grating of rectangular profile (of period d, groove width a, and groove depth l) shown in Fig. 6. Evidently, if the charge moves so that it almost touches the peaks of the grating, then the effective dipole moment is $2\epsilon l$ during the time a/u (while passing over a groove), and zero during the time (d − a)/u (while passing over a peak). If we expand the dipole moment in a Fourier series:

$$p(t) = \sum p_n e^{2\pi i \frac{u}{d} nt}, \tag{20}$$

and calculate the amplitude of the first harmonic, we get

$$|p_1| = \frac{2\epsilon l}{\pi}\sin\frac{\pi a}{d}. \tag{21}$$

We must substitute this quantity as p into (19) in order to estimate the intensity of the first-order spectrum. As we see, the effective dipole moment is of the order of magnitude of ϵl (if we consider that $\sin \pi a/d \approx 1$).

We note that the effective-dipole model does not give an exponential dependence of the emission intensity on the impact parameter b. Hence, it can be applied only for small values of b.

When the diffraction grating is a slightly corrugated metal surface, we can use perturbation theory to calculate the field excited by the moving source. Let us assume that we know the solutions of the field equations satisfying the boundary conditions for the given ideally-conductive surfaces. Then, if the surfaces are slightly deformed, it turns out that we can express the variations in the field thus arising in terms of the displacement of the surface at each point. The corresponding formula has the form[11,12]

$$\Delta H = \frac{i\omega}{4\pi}\int_{S_0}(E_n^0 E_n' + H_t^0 H_t')\,h(S)\,dS. \tag{22}$$

Here ΔH is the variation in the field that arises when the surface S_0 is displaced by the amount h(S); E^0 and H^0 are the fields satisfying the boundary conditions for the undistorted surface S_0; E′ and H′ are the fields of an auxiliary unit dipole situated at the point of observation. The subscripts n and t denote the components of the field respectively normal and tangential to the undistorted surface S_0. V. N. Parygin[13] has calculated the emission intensity by using perturbation theory. Conveniently, one chooses a plane as the surface S_0. Let a planar modulated electron flux pass above an ideally conductive plane situated at y = 0, the current density being given by the formula

$$j = j_0\delta(y-b)\,e^{i\frac{\omega}{u}(z-ut)} \tag{23}$$

(b is the distance from the current of particles to the surface of the metal). In this problem, the field satisfying the assigned boundary conditions at the plane y = 0 can be found without trouble. Now let us deform the surface S_0 by a harmonic law. That is, we shall displace the surface at each given point z by the amount

$$h(z) = h\sin\frac{2\pi}{d}z. \tag{24}$$

Then we can find by Eq. (22) the fraction of the field excited as the planar modulated beam moves above the corrugated surface:

$$\begin{aligned}\Delta H = {} & \frac{2\pi j_0 h}{c}\,\frac{\frac{\omega}{u}\left(\frac{\omega}{u}+\frac{2\pi}{d}\right)-\frac{\omega^2}{c^2}}{\sqrt{\left(\frac{\omega}{u}+\frac{2\pi}{d}\right)^2-\frac{\omega^2}{c^2}}}\exp\left\{-\sqrt{\frac{\omega^2}{u^2}-\frac{\omega^2}{c^2}}\,b\right. \\ & \left.-\left[\sqrt{\left(\frac{\omega}{u}+\frac{2\pi}{d}\right)^2-\frac{\omega^2}{c^2}}\,y+i\left(\frac{\omega}{u}+\frac{2\pi}{d}\right)z-i\omega t\right]\right. \\ & -\frac{2\pi j_0 h}{c}\,\frac{\frac{\omega}{u}\left(\frac{\omega}{u}-\frac{2\pi}{d}\right)-\frac{\omega^2}{c^2}}{\sqrt{\left(\frac{\omega}{u}-\frac{2\pi}{d}\right)^2-\frac{\omega^2}{c^2}}}\exp\left\{-\sqrt{\frac{\omega^2}{u^2}-\frac{\omega^2}{c^2}}\,b\right. \\ & \left.\left.+i\left[\sqrt{k^2-\left(\frac{\omega}{u}-\frac{2\pi}{d}\right)^2}\,y+\left(\frac{\omega}{u}-\frac{2\pi}{d}\right)z-\omega t\right]\right\}.\end{aligned} \tag{25}$$

The first term in the obtained expression for the excited field defines a surface wave propagated along the corrugated surface at a somewhat slower speed than the wave in the source current. This term cannot describe a propagated field, since it declines exponentially with increasing y. Under certain conditions, the second term can describe a propagated wave. Radiation is possible if the velocity of the current wave and the period of the structure satisfy the inequalities (15), where we must take m = 1. Thus, Eq. (25) describes the first-order emission spectrum. The higher orders in the emission spectrum cannot be described in this approximate calculation (which is linear in the perturbation of the surface). As we see from the expression for the excited

field, the emission intensity sharply (exponentially) declines with increasing impact parameter. When $k \approx \pm[(\omega/u) - (2\pi/d)]$ (i.e., near the limits of the region of emission of the first space harmonic of the field), the amplitude of the field determined from Eq. (25) increases greatly, and thus the limits of applicability of the perturbation theory are exceeded.

A recently-published study[14] has also discussed on the basis of perturbation theory the problem of emission from sources moving close to an open periodic structure having a profile of very general form.

The Kirchhoff Approximation

In deriving Eq. (2) for the emission spectrum of a charge above a diffraction grating, we used simple thinking based on Huyghen's principle. It is natural to try to apply the same thinking also to calculate the emission intensity. This has been done in[15] for the case of a plane transparent diffraction grating. In distinction from a reflecting grating, this grating consists of parallel metal strips lying in one plane and separated by slits (see Fig. 2). Let the slit width of the grating be a. Then the width of a strip is d – a, where d is the period of the grating. According to Huyghens' principle, when the charge moves above the grating, the field in the space below the grating is determined by the values of the field at the slits in the plane of the grating. If we neglect the vector nature of the electromagnetic field, then the values of the field below the grating are related to its values at the slits by the well-known Huyghens–Kirchhoff relation, which is widely used in the scalar theory of diffraction:

$$g(x, y, z) = \int \frac{kg_0(x', 0, z')}{2\pi i R} e^{ikR}\, dS_n. \tag{26}$$

Here $k = \omega/c$; g_0 and g are the spectral components of the field functions corresponding to the frequency ω; R is the distance between the observation point and the integration point; dS_n is the product of the element of area dS and the cosine of the angle between the ray of incident light and the normal to the surface:

$$dS_n = dS\left(\mathbf{n}\frac{\mathbf{k}}{k}\right), \tag{27}$$

where **k** is the wave vector of the wave incident on the aperture. The integration is performed over the gaps (slits) in the plane of the grating. Here we assume that the field g in the apertures in the screen is given by the same expression as in the absence of a screen. Let a particle of charge ϵ move at constant velocity u at a distance l above the grating in a direction parallel to the z axis. We shall describe the field of the freely-moving charge by the scalar function

$$g_0(x, y, z) = A_{z\omega}(x, y, z), \tag{27'}$$

where $A_{z\omega}$ is the Fourier coefficient of the component of the vector potential along the z axis. $A_{z\omega}$ has the following form in the plane of the grating (y = 0):

$$g_0(x, 0, z) = A_{z\omega}(x, 0, z) = \frac{i\varepsilon}{2\pi c}\int \frac{dk_x}{\sigma(k_x, \omega)} e^{i\left(\sigma b + k_x x + \frac{\omega}{u} z\right)}, \tag{28}$$

where

$$\sigma(k_x, \omega) = \sqrt{(\beta^2 - 1)\frac{\omega^2}{u^2} - k_x^2} = k_y \tag{29}$$

is the projection of the wave vector of the incident wave on the y axis. Let us substitute the expression (28) for $g_0(x, 0, z)$ into Eq. (26). Then the vector potential of the diffracted field will have the following form (in the region of the wave at great distances R_0 from the grating):

$$g(x, y, z) = -\frac{\varepsilon a}{c}\frac{e^{ikR_0}}{R_0}\frac{\sin\frac{a}{2}\left(\frac{\omega}{u} - k_z\right)}{\frac{a}{2}\left(\frac{\omega}{u} - k_z\right)} e^{i\sigma b + i\left(\frac{\omega}{u} - k_z\right)\frac{a}{2}} \sum_{n=-\infty}^{\infty} \delta\left[\left(\frac{\omega}{u} - k_z\right)d - 2\pi n\right]. \tag{30}$$

The presence of the δ function in Eq. (30) corresponds to the previously-discussed relation (2) that the emission from the charge passing above the grating must satisfy. In fact, since $k_z = (\omega/c)\cos\theta$, the condition that the argument of the δ function should vanish is equivalent to Eq. (2). The given frequency is missing in other directions of emission.

If we know the vector potential of the emission field, we can calculate the emission energy occurring in the frequency interval from ω to $\omega + d\omega$ for the solid angle $d\Omega$:[8]

$$dW_\omega = ck^2 |g|^2 R_0^2 \sin^3\theta\, d\varphi\, d\omega \tag{31}$$

(φ is the angle between the negative y axis and the projection of the wave vector on the xy plane). In this formula g is determined by Eq. (30). After simple transformations, we get

$$dW_\omega = \frac{\varepsilon^2 a^2 k^2}{2\pi c}\frac{uT}{d}\frac{\sin^2\frac{a\omega}{2u}(1 - \beta\cos\theta)}{\left[\frac{a\omega}{2u}(1 - \beta\cos\theta)\right]^2} e^{-2b\frac{\omega}{u}\sqrt{1 - \beta^2(1 - \sin^2\theta\sin^2\varphi)}} \times \sum_n \delta\left[\frac{\omega}{u}(1 - \beta\cos\theta)\, d - 2\pi n\right]\sin^3\theta\, d\theta\, d\varphi\, d\omega, \tag{32}$$

where the summation is performed over the values of the order n corresponding to the emitted spectral lines (see the inequality (13)), and T is the time of flight of the charge above the grating.

We can obtain the spectral distribution of the emission energy corresponding to the n-th line in the angular interval $d\varphi$ by integrating Eq. (32) over the angle θ:

$$dW_{n,\omega} = \frac{\varepsilon^2}{2\pi c} kL\left(\frac{\sin n\pi\frac{a}{d}}{n\pi}\right)^2 \times \exp\left\{-2bk\sqrt{\gamma^2 + \left[1 - \left(\frac{1}{\beta} - \frac{2\pi n}{kd}\right)^2\right]\sin^2\varphi}\right\} d\omega\, d\varphi. \tag{33}$$

Here L is the length of the diffraction grating.

If we integrate (32) over the frequency, we get the angular distribution of losses for the n-th spectral line:

$$dW_n(\theta, \varphi) = \frac{2\pi\varepsilon^2 a^2}{c^3}\frac{uT}{d}\left(\frac{u}{d}\right)^3\left(\frac{\sin n\pi\frac{a}{d}}{\pi\frac{a}{d}}\right)^2 \times \exp\left\{-\frac{4\pi n b}{d(1 - \beta\cos\theta)}\sqrt{1 - \beta^2(1 - \sin^2\theta\sin^2\varphi)}\right\}\frac{\sin^3\theta\, d\theta\, d\varphi}{(1 - \beta\cos\theta)^3}. \tag{34}$$

We see from the derived formulas that the emission intensity declines exponentially with increasing distance of the source from the plane of the grating. Here the exponent of decline of intensity is proportional to the order of harmonic of the emission.

One can also calculate the emission for the discussed model of a plane transparent grating by the following visually-obvious method. An observer located above the grating can see a charge moving below the grating only

in the intervals of time when it is alongside the slits. Hence the motion of the charge will seem non-uniform to the observer: for the observer, the charge appears at the edge of a slit and disappears at its other edge after the time a/u, and then it appears at the next slit after the time (d − a)/u. The current associated with the charge will then differ from zero for values of the time t defined by the inequality

$$\frac{md}{u} \leqslant t \leqslant \frac{md+a}{u}, \tag{35}$$

where m is any integer, positive or negative. The emission from a charge moving according to such a law in vacuo can be determined by using the well-known formula:[8]

$$\mathbf{A}_\omega = \frac{e e^{ikR_0}}{2\pi c R_0} \int \mathbf{u}(t)\, e^{i[\omega t - \mathbf{kr}(t)]}\, dt, \tag{36}$$

where $\mathbf{A}_\omega$ is the Fourier component of the vector potential, $\mathbf{r} = \mathbf{r}(t)$ is the law defining the motion of the point charge, and $\mathbf{u}(t) = d\mathbf{r}/dt$.

If we integrate (36) over the intervals determined by the inequality (35), and use the obtained expression to determine the emission intensity, we arrive at expressions that differ from Eqs. (32)—(35) only in lacking the exponential factor. Thus, if the impact parameter b is small in comparison with the absolute value of $1/\sigma$ (see Eq. (29)), then both methods give the same results (the quantity σ defines the distance at which the field of the source declines by a factor of e). However, if the impact parameter b is large, Eq. (36) cannot be applied, since it takes no account of diffraction effects at the edges of the strips. These effects have the result that the charge seems to become visible to the observer at an earlier instant of time than md/u, and passes from the field of view at an instant of time later than (md + a)/u. Thus, diffraction at the edges of the strips makes the choice of limits of integration in (36) indefinite. As the trajectory of the charge becomes more distant from the grating, this indefiniteness increases, and use of Eq. (36) to calculate the characteristics of the emission is ruled out.

From the results obtained for a point charge, we can easily derive the solution for the two-dimensional problem in which the field source is an infinite uniformly-charged filament or a modulated plane electron wave. In this case, the radiation field is defined by the formula

$$g(y, z) = \frac{k}{2} \int_\Sigma g(0, z')\, H_0^{(1)}(kR')\, dz', \tag{37}$$

where

$$R' = \sqrt{y^2 + (z - z')^2}.$$

As the function g(0, z) we must take

$$A_{z\omega}(x, 0, z) = \frac{\varepsilon}{\omega\nu} e^{-k\gamma b + i\frac{\omega}{u}z}, \tag{38}$$

where ε is the linear charge density of the linear source. Equations (37) and (38) are derived from (26) and (28), respectively, by integrating over the transverse coordinate x.

The vector potential of the diffracted field in the two-dimensional problem takes on the form

$$A_{z\omega}(y, z) = \varepsilon a \sqrt{\frac{2\pi}{\omega c}} \frac{\sin\frac{ka}{2\beta}(1-\beta\cos\theta)}{\frac{ka}{2\beta}(1-\beta\cos\theta)} \frac{e^{ikR_0 + i\frac{\pi}{4}}}{\sqrt{R_0}}$$

$$\times e^{-k\gamma b + i\frac{ka}{2\beta}(1-\beta\cos\theta)} \sum_n \delta\left[d\left(\frac{\omega}{u} - k\cos\theta\right) - 2\pi n\right]. \tag{39}$$

Using this expression for the emission losses per unit length as the charged filament passes close to the plane grating, we get

$$dW_{\omega, n} = ck^2 |A_{z\omega}|^2 \sin^2\varphi R\, d\varphi = \varepsilon^2 ka \frac{u}{c}\frac{a}{d} T \sin^2\theta \left|\frac{\sin\frac{ka}{2\beta}(1-\beta\cos\theta)}{\frac{ka}{2\beta}(1-\beta\cos\theta)}\right|^2$$

$$\times e^{-2k\gamma b} \sum_n \delta\left[d\left(\frac{\omega}{n} - \cos\theta\right) - 2\pi n\right] d\theta. \tag{40}$$

The cited formulas have been derived by means of the scalar theory of diffraction, in which the field is described by a single scalar function. However, the scalar function does not completely describe the vector electromagnetic field. In particular, the scalar diffraction theory proves inadequate to determine the polarization of the emission field of a charge moving above a diffraction grating. We can generalize the above approximate treatment by using the vector electrodynamic formulation of the Huyghens—Kirchhoff principle to calculate the field emitted by the charge. According to this formulation, the scattered field is described by two vector functions $\mathbf{A}^e$ and $\mathbf{A}^m$ determined by the electric and magnetic fields $\mathbf{E}^0$ and $\mathbf{H}^0$ incident at the aperture e of the screen:

$$\mathbf{A}^e = \frac{1}{4\pi}\oint_\Sigma \frac{e^{ikR}}{R}[\mathbf{nH}^0]\, dS, \quad \mathbf{A}^m = -\frac{1}{4\pi}\oint_\Sigma \frac{e^{ikR}}{R}[\mathbf{nE}_0]\, dS, \tag{41}$$

where $\mathbf{n}$ is the normal to the plane of the aperture, and Σ is the area of the aperture. In this case, Eq. (41) supplants the corresponding scalar relation (26).

The fields $\mathbf{E}$ and $\mathbf{H}$ are defined in terms of $\mathbf{A}^e$ and $\mathbf{A}^m$ by the well-known formulas

$$\mathbf{E} = -\frac{1}{ik}(\operatorname{grad}\operatorname{div}\mathbf{A}^e + k^2\mathbf{A}^e) - \operatorname{rot}\mathbf{A}^m,$$
$$\mathbf{H} = \operatorname{rot}\mathbf{A}^e - \frac{1}{ik}(\operatorname{grad}\operatorname{div}\mathbf{A}^m + k^2\mathbf{A}^m). \tag{42}$$

If we substitute into (41) the values of the field of a uniformly-moving charge and take the slits of the grating as the surface over which the integration is performed, we obtain the radiation field from (42). V. I. Gaĭduk and B. M. Bolotovskiĭ have undertaken such calculations.

The calculations give the following formulas for the non-zero components of the vectors $\mathbf{A}^e$ and $\mathbf{A}^m$:

$$\left.\begin{aligned} A_z^e &= -i\beta B, \\ A_x^m &= \frac{\omega}{u\sigma}(1-\beta^2)B, \\ A_z^m &= \frac{k_x}{\sigma}B, \end{aligned}\right\} \tag{43}$$

where σ is determined by Eq. (29), and

$$B = \frac{\varepsilon}{u}\frac{e^{ikR}}{R} e^{-\sigma b + i\frac{\omega}{u}\frac{a}{2}(1-\beta\cos\theta)}$$

$$\times \frac{\sin\frac{\omega}{u}(1-\beta\cos\theta)\frac{a}{2}}{\frac{\omega}{u}(1-\beta\cos\theta)} \sum_n \delta\left[\frac{\omega}{u}(1-\beta\cos\theta)\, d + 2\pi n\right]. \tag{44}$$

*$[\mathbf{n}\,\mathbf{H}^0] \equiv \mathbf{n} \times \mathbf{H}^0$.

Equations (43) and (44) determine the spectral components of the vectors $\mathbf{A}^e$ and $\mathbf{A}^m$ corresponding to the frequency ω. The fields **E** and **H** are expressed in terms of $\mathbf{A}^e$ and $\mathbf{A}^m$ by the formulas of (42). We get the following expression for the emitted energy:

$$dW_\omega = \frac{\varepsilon^2 a^2}{8\pi c} k^2 \frac{uT}{d} \left[\frac{\sin \frac{a\omega}{2u}(1-\beta\cos\theta)}{\frac{a\omega}{2u}(1-\beta\cos\theta)} \right]^2 e^{-2b\frac{\omega}{u}\sqrt{1-\beta^2(1-\sin^2\theta\sin^2\varphi)}} \times \left\{ \sin^2\theta + \frac{1}{\beta^2} \frac{\beta^2\sin^2\theta\cos^2\varphi + (1-\beta^2) - \sin^2\theta\cos^2\varphi\,[\beta\cos\theta - (1-\beta^2)]^2}{1-\beta^2(1-\sin^2\theta\cos^2\varphi)} \right\} \times \sum \delta\left[\frac{\omega}{u} d(1-\beta\cos\theta) - 2\pi n\right] \sin\theta\, d\theta\, d\varphi\, d\omega. \quad (45)$$

As we see from eqs. (43)—(45), the vector formulation of Huyghens' principle indicates that the polarization and angular distribution of the emission are more complex in nature. However, the emission intensity given by the scalar theory proves to be of the same order of magnitude as in the vector theory over a considerable angular range.

Similar assumptions were used in [16] to calculate the emission intensity of a charged particle moving over a diffraction grating.

III. EXACT SOLUTIONS OF THE PROBLEM OF EMISSION FROM A SOURCE IN THE VICINITY OF A GRATING

The models of diffraction gratings studied above resembled actual configurations, but did not admit of exact treatment. Hence, in each case we had to base the solution on various physical assumptions that simplified calculation. It is of great interest to seek exact solutions of the problem that permit us more completely to discern the pattern of the phenomenon and to estimate the limits of applicability of the derived approximate results. We can derive such solutions only in rare cases, usually with extremely idealized models of the diffraction grating.

1. Emission from a Modulated Electron Current Close to an Impedance Plane

Hessel [17] has discussed a very simple problem of the type cited above. The diffraction grating is a surface whose optical properties vary from point to point. We can characterize the properties of this surface by fixing at each point the ratio of the tangential components of the electric and magnetic fields:

$$\frac{E_t}{H_t} = \zeta. \quad (46)$$

The quantity ζ is called the impedance of the surface. Assignment of a surface impedance is appropriate both for good conductors and for approximating the properties of rough surfaces, provided that the characteristic period of the roughness is small in comparison with the wavelength of the electromagnetic field. In [17] the diffraction grating was approximated by a plane y = 0 having a periodically-varying purely reactive impedance

$$\zeta(z) = -iX_s\left(1 + M\cos\frac{2\pi}{a}z\right), \quad (47)$$

where M and a are respectively the degree of modulation and the period, and X_S is the value of the constant component of the impedance. The electromagnetic field created by a plane modulated electron beam having a charge density distribution defined by

$$\rho(\mathbf{r}, t) = \rho_0\left[1 + \alpha\cos\frac{k}{\beta}(z - ut)\right]\delta(y - b),$$

lying parallel to the described impedance plane can be expressed as a superposition of space harmonics:

$$H(y, z) = e^{i\frac{k}{\beta}z} \sum_{n=-\infty}^{\infty} I_n e^{i\frac{2\pi}{a}nz} e^{i\sqrt{k^2 - \left(\frac{k}{\beta} + \frac{2\pi}{a}n\right)^2}\,y}. \quad (48)$$

Each of the partial plane waves either behaves as a surface wave declining exponentially as we go away from the y = 0 plane, or it propagates without decay, depending on the relation between the phase velocity β = u/c of the modulation wave and the period of the impedance variation. In the latter case, the direction of propagation of a plane harmonic is related to the grating period, the frequency, and the velocity of the beam by the previously-derived Eqs. (1) and (12). If we require that the overall field should satisfy the impedance boundary conditions (46) and (47) at the surface of the "grating," we obtain a system of recurrent equations for the amplitudes of the plane space harmonics I_n. We can derive expressions in the form of continuous fractions amenable to numerical analysis from this system of equations for the amplitudes I_n. Study shows that the variation of I_n as a function of the variable k/β for a given value of the parameter ka shows sharply marked resonance maxima. Figure 7 shows a typical example of a resonance variation of the I_n coefficients, as taken from [17]. The diagram shows two amplitudes I_n corresponding to n = −1 and n = −2. With the chosen values of the parameters (ka = 1.6π, M = 0.2, X_S = 1, ka/4.64π < β < ka/3.52π), the amplitude I_{-1} corresponds to a damped wave, while the amplitude I_{-2} defines an undamped emission wave. We see that both amplitudes have a sharp maximum at kd/β = 4.26π.

The characteristic behavior of the I_n (k/β) curves near the maxima is analogous to the breaks in the spectral variations of the reflectivity of a periodic strip grating for a plane homogeneous wave (see, e.g., Sec. 52 in [18]). Wood was the first to observe such sharp contrasts in the intensity distribution in a diffraction spectrum, and they are sometimes called "Wood anomalies." This effect has been treated qualitatively in [39], where

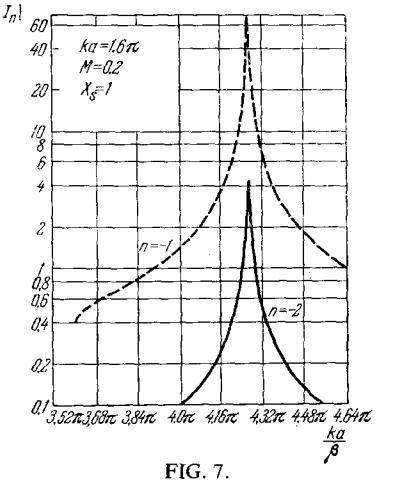

FIG. 7.

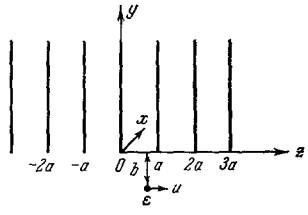

FIG. 8.

the sharp variation of intensity in the diffraction spectrum was related to the appearance of new diffraction spectrum lines. Analogously, the point in the relation of the wave number k to the source velocity β at which the emission intensity of the observed space harmonic drops sharply (the break in the I_n (k/β) curve) corresponds to the condition of appearance of a new propagated space harmonic.

2. The Emission from a Charged Filament and from a Point Charge Passing Close to a Periodic Structure Consisting of Ideally-conductive Half-planes

Another simple model of a diffraction grating permitting exact analytical study is a periodic system of uniformly-spaced ideally conductive thin half-planes (Fig. 8). The electromagnetic field of an emission source in passing near such a structure can be determined by the Wiener-Hopf-Fock method.[18,19] The review[2] contains a detailed treatment of this method (see also[20-23]). The same review describes the determination of a solution for the case in which the emission source is a uniformly charged filament moving past the structure. An analytic solution of the problem was also derived in[22] for the case in which the emission source is a point charge. We shall be concerned below mainly with analyzing the obtained quantitative results.*

1) When the source is a uniformly-charged filament (or a plane modulated electron beam), the electromagnetic field is completely described by a single non-zero component of the magnetic field defined by the following expressions:

$$H_{x\omega}=\begin{cases}\sum\limits_{m=0}^{\infty} R_m\cos\frac{m\pi}{a}z e^{iw_m y} & \text{if} \quad y>0,\\ H^0_{x\omega}+\sum\limits_{m=-\infty}^{\infty} Q_m e^{i\left(\frac{\omega}{u}-\frac{2\pi}{a}m\right)z+i\hat{w}_m y} & \text{if} \quad y<0.\end{cases} \tag{49}$$

The field in each of the plane waveguides forming the structure (y > 0, an ≤ z ≤ a(n + 1)) consists of a set of waveguide harmonics propagated inward from the open end. The excitation coefficients R_m of these normal modes of the waveguide are determined by the formulas

$$R_m=\alpha_m(-1)^{mn}\frac{2\varepsilon k\gamma e^{-k\gamma b+i\frac{\omega}{u}an}}{ua(1+i\gamma)}\frac{L_1(w_m)}{L_1(ik\gamma)}\frac{(k+w_m)[1-(-1)^m e^{i\frac{h}{\beta}a}]}{w_m(w_m^2+k^2\gamma^2)};$$

where

$$\alpha_m=\begin{cases}-1/2 & \text{where } m=0,\\ 1 & \text{where } m\geqslant 1,\end{cases}\qquad \gamma=\frac{\sqrt{1-\beta^2}}{\beta},$$

$$w_m=\sqrt{k^2-\left(\frac{m\pi}{a}\right)^2} \tag{50}$$

*The quantitative results described in this and in following sections were obtained by E. V. Avdeev and G. V. Voskresenskiĭ.

are the propagation constants of the waveguide harmonics.

The functions $L_1(w)$ occurring in (50) and the associated functions $L_2(w)$ are expressed explicitly as infinite products by the formulas*

$$L_{1,2}(w)=\sqrt{\frac{\gamma^2}{2}\frac{ka\sin ka}{\cos ka-\cos\frac{ka}{\beta}}}\,e^{\mp i\frac{wa}{\pi}\ln 2}\prod_{m=1}^{\infty}\frac{\left(1\pm\frac{w}{w_m}\right)}{\left(1\pm\frac{w}{w_m}\right)\left(1\pm\frac{w}{\hat{w}_{-m}}\right)}. \tag{51}$$

The upper sign in the factors corresponds to the subscript 1 in the function being defined, and the lower sign to the subscript 2.

The field in free space is represented as the sum of the intrinsic field $H^0_{x\omega}$ of the source moving in vacuo and a surface wave of amplitude Q_0 propagated along the structure synchronously with the source, and also as a superposition of harmonics of amplitudes Q_m and wave vectors

$$k_{zm}\equiv\hat{v}_m=\frac{\omega}{u}-\frac{2\pi}{a}m,\quad k_{ym}\equiv\hat{w}_m=\sqrt{k^2-k_{zm}^2}. \tag{50a}$$

The amplitudes of the harmonics of the field in free space are expressed by the formulas

$$Q_0=-\frac{\varepsilon c e^{-k\gamma b}}{u^2(1+i\gamma)^2}\frac{L_1(-ik\gamma)}{L_1(ik\gamma)},$$

$$Q_m=\frac{ik\gamma\varepsilon e^{-k\gamma b}}{u(1+i\gamma)L_1(ik\gamma)}\frac{1}{\hat{w}_m}\frac{\frac{2\pi}{a}m-\frac{\omega}{u}}{L_2(-\hat{w}_m)}\frac{1}{k+\hat{w}_m}$$
$$(m=\pm 1,\ \pm 2,\ \pm 3). \tag{50b}$$

Depending on the value of the projection of the wave vector $k_{ym}=\hat{w}_m$, the harmonics can behave as surface waves (exponentially decaying as we go away from the edge of the structure) or may represent emitted plane waves (for real $\hat{w}_m$). The requirement that $\hat{w}_m$ should be real coincides with the conditions (12) and (15) derived above.

We can determine the overall energy losses by emission from a charged filament in uniform motion by calculating the reaction of the radiation, i.e., the work done on the source by the emitted field per unit path*:

$$\frac{dW}{dz}=-2\mathrm{Re}\int_0^{\infty}\varepsilon E_{z\omega}(z=ut,\ y=-b)e^{-i\omega t}d\omega=\int_0^{\infty}\frac{dW_\omega}{dz}d\omega, \tag{52}$$

where ε is the linear charge density of the filament. According to (49), (51), and (52), we obtain the following expression for the spectral density of losses as the source passes over one period of the structure (0 ≤ z ≤ a):

$$W_\omega^{\mathrm{tot}}=\frac{2\varepsilon^2\gamma a}{u\beta}e^{-2k\gamma b}\mathrm{Re}\left\{\frac{i}{(1+i\gamma)^2}\frac{L_1(-ik\gamma)}{L_1(ik\gamma)}\right\}$$
$$=-\frac{4\varepsilon^2 a(1-\beta^2)}{c|L_1(ik\gamma)|^2}e^{-2k\gamma b}\left\{\mathrm{Re}\,A+\frac{\gamma^2-1}{\gamma}\mathrm{Im}\,A\right\}, \tag{53}$$

where the quantity A is expressed in terms of the finite products:

$$A=\prod_n\frac{k\gamma+iw_n}{k\gamma-iw_n}\prod_m\frac{k\gamma-i\hat{w}_m}{k\gamma+i\hat{w}_m}, \tag{54}$$

*Here we take the opportunity to correct an error made in defining the functions $L_{1,2}(w)$ in [20-23]. Introduction of the exponential factor $\exp[\mp i(wa/\pi)\ln 2]$ ensures correct asymptotic behavior of the functions. Furthermore, writing the functions $L_{1,2}(w)$ in the more symmetric form of (51) is more convenient for making calculations.

†The expressions (52) and (53) for a two-dimensional source define the losses per unit length of filament.

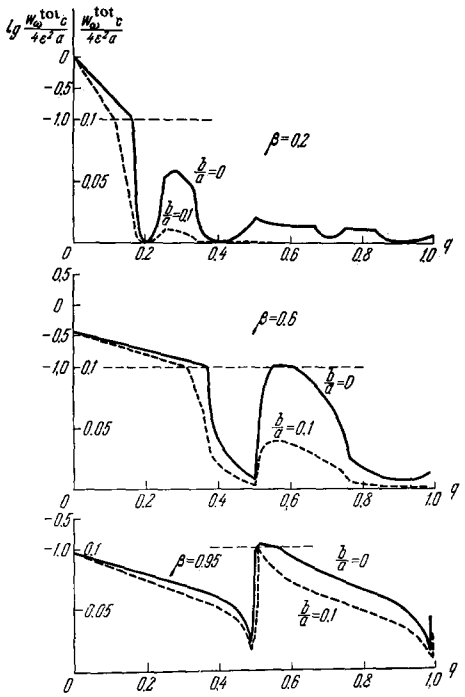

FIG. 9.

where the factors contain only the wave numbers w_n and $\hat{w}_m$, which are purely real (for the given values of the frequency and velocity). Equation (53) can be greatly simplified in various special cases. Thus, when only a TEM wave ($ka \leq \pi$) can be propagated in a waveguide cell, and the emission into free space involves only the first space harmonic, the spectral density of losses per period acquires the form

$$W_\omega^{tot} = \frac{\varepsilon^2 a}{\pi c}\frac{1-\beta^2}{|L_1(ik\gamma)|^2}e^{-2k\gamma b}\frac{(\hat{w}_1^2-k^2\gamma^2)-(1-\gamma^2)k\hat{w}_1}{\frac{\pi}{a}-\frac{k}{\beta}}. \qquad (53')$$

A quantitative analysis was performed of the spectral density of losses as a function of the velocity β of the filament and the emission frequency for various values of the impact parameter. For illustration, Fig. 9 shows curves of $W_\omega^{tot}/(4\epsilon^2 a/c)$ as a function of the dimensionless frequency $q = ka/2\pi \equiv a/\lambda$ for three values of the velocity β (0.2, 0.6, and 0.95) for b/a = 0 and 0.1. We note that the radiation reaction vanishes when $q = n\beta$. This corresponds to the absence of losses by emission at frequencies that are multiples of the "frequency of passage" of a period of the structure (see also[2], p. 244).

When the parameters of the problem satisfy the relation $2\pi q\gamma b/a \gtrsim 1$, we can describe the spectral distribution of losses rather precisely by the exponential factor in (53) alone. Here, by integrating over the frequencies, we can derive a very simple approximate expression for the overall losses of energy from the charged filament:

$$W = 2\varepsilon^2\beta^2\gamma\frac{a}{b+\frac{\ln 2a}{\pi}} \equiv 2\varepsilon^2\beta^2\gamma\frac{a}{b_{red}}. \qquad (55)$$

The derived approximate estimate holds in two limiting cases. For low velocities of the filament ($\gamma \approx 1/\beta$), the emission is mainly concentrated in the low-frequency region; then the overall losses are proportional to the velocity of the source. For ultrarelativistic velocities of the filament ($\beta \approx 1$), the emission covers a wide range reaching up to very high frequencies; then the overall losses are inversely proportional to the energy of the source. In both cited cases, the overall losses are inversely proportional to the impact parameter of the source (b_{red}/a). Figure 10 shows the overall losses of the source as a function of the velocity for two values of the impact parameter, $b_{red}/a = 1/3$ and 2/3 (b_{red} is the reduced value of b). These curves were obtained by integrating the exact expression (53) for the losses over the frequency. We see that the initial and final portions of the curves in Fig. 10 are well described by the approximate expression (55).

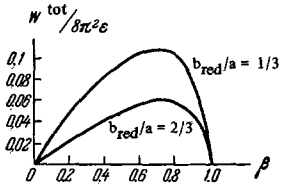

FIG. 10.

Let us determine the emission losses into the free half-space from the flux of energy through a plane parallel to the edge of the structure (x, z), and lying below the trajectory of the source ($y < -b$). If we calculate the flux of the Poynting vector through a strip of width a in this plane, we obtain the sought spectral density of losses per period of the structure:

$$W_\omega^{free} = -\frac{4\varepsilon^2 a}{c}\frac{(1-\beta^2)}{|L_1(ik\gamma)|^2}e^{-2k\gamma b}\frac{q}{\beta^2}\sum_m \frac{\hat{w}_m}{1-\frac{2q}{m\beta}}\frac{q-\hat{w}_m}{q+\hat{w}_m}A_m(q,\beta),$$

$$A_m = \prod_n\prod_l \frac{\hat{w}_m-w_n}{\hat{w}_m+w_n}\frac{\hat{w}_m+\hat{w}_l}{\hat{w}_m-\hat{w}_l}. \qquad (56)$$

The summation in (56) is extended only over values of the subscript m corresponding to emitted space harmonics, while the function $A_m(q, \beta)$ is analogous in nature to the quantity A in Eq. (53). We shall also give a simple expression for the losses in the case in which only the first harmonic can be emitted ($\beta/(1+\beta) \leq q \leq 1/2$):

$$W_\omega^{free.\,1} = -\frac{4\varepsilon^2 a\pi\gamma^2}{c|L_1(ik\gamma)|^2}e^{-2k\gamma b}\frac{k\hat{w}_1(k-\hat{w}_1)^2}{\left(\frac{k}{\beta}-\frac{2\pi}{a}\right)^2\left(\frac{\pi}{a}-\frac{k}{\beta}\right)}. \qquad (56')$$

We can illustrate the characteristics of the emission into the free half-space by the spectral distributions of the first-harmonic intensity shown in Fig. 11 for different velocities of the source (β = 0.15, 0.3, 0.4, 0.6, and 0.8). As we see, the emission is concentrated into two frequency ranges. Here the intensity of the high-frequency Lobe declines considerably with increasing velocity. In addition, the emission region is shifted to higher frequencies with increasing velocity of the source (the high-frequency Lobe is especially greatly shifted). Here the fore-and-aft asymmetry of emission becomes even more evident. Figure 12 shows in polar coordinates the curves of the angular distribution of the emission intensity of the first space harmonic. At low source velocity, the angular distribution of the emission intensity is described by a smooth two-lobed directional diagram. With increasing filament velocity, in accordance with the increasing complexity of the emission field, the

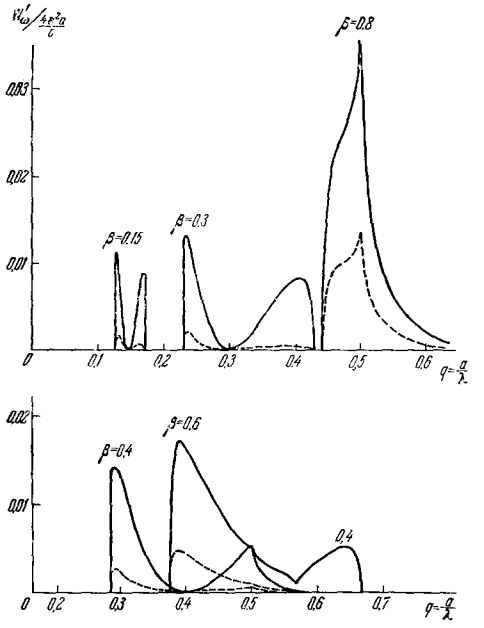

FIG. 11.

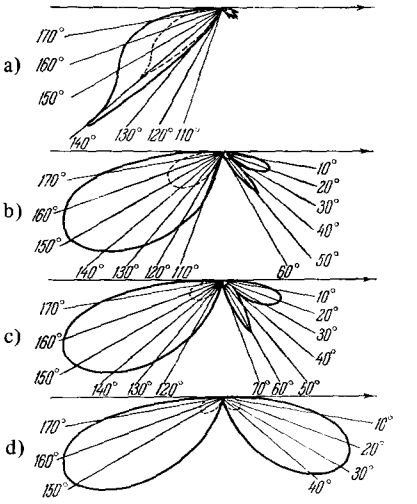

FIG. 12. Directional diagrams of emission of the first space harmonic for two values of the impact parameter: b/a = 0 – solid curve; b/a = 0.1 – dotted curve. The direction of motion of the source is shown by the arrow arrow. a) $\beta = 0.08$; b) $\beta = 0.6$; c) $\beta = 0.4$; d) $\beta = 0.15$.

lobes of the directional diagram begin to be separated, each gap corresponding to the onset of excitation of the next waveguide harmonic.

In analogy to the determination of the emission into the free half-space, we can calculate the energy flux emitted into a waveguide cell of the periodic structure. As we can verify, the total losses by emission and the work done by the radiation field on the source satisfy a balance equation here. This serves to confirm the correctness of the derived analytical expressions for the losses.

2) If the emission source is a point charge rather than a charged filament, all the components of the vectors of the electromagnetic field are non-zero. In this case, one can[22] reduce the mathematical formulation of the problem to solving a system of four "paired" integral equations for the unknown current distributions on the plates of the retarding structure:

$$E_{x\omega}(\mathbf{r}) = \frac{\varepsilon e^{-i\frac{\pi}{4}}}{\sqrt{2\pi r}\,u}\sum_{m=-\infty}^{\infty}\frac{e^{-b\sqrt{k^2\gamma^2+\hat{w}_m^2\sin^2\varphi}}}{L_1\left(i\sqrt{k^2\gamma^2+\hat{w}_m^2\sin^2\varphi}\right)}\frac{\hat{w}_m^{1/2}\sin\varphi}{L_2(\hat{w}_m\cos\varphi)}e^{i\hat{w}_m r+i\hat{v}_m z},$$

$$H_{x\omega}(\mathbf{r}) = -\frac{ike e^{-i\frac{\pi}{4}}}{\sqrt{2\pi r}\,u}\sum_{m=-\infty}^{\infty}\frac{e^{-b\sqrt{k^2\gamma^2+\hat{w}_m^2\sin^2\varphi}}}{L_1\left(i\sqrt{k^2\gamma^2+\hat{w}_m^2\sin^2\varphi}\right)}\frac{1}{\hat{w}_m^{1/2}L_2(\hat{w}_m\cos\varphi)}$$

$$\times\frac{\hat{v}_m\sqrt{k^2\gamma^2+\hat{w}_m^2\sin^2\varphi}\,e^{i\hat{w}_m r+i\hat{v}_m z}}{\left[\hat{w}_m\cos\varphi-\sqrt{k^2\cos^2\varphi+\hat{v}_m^2\sin^2\varphi}\right]\left[\sqrt{k^2\cos^2\varphi+\hat{v}_m^2\sin^2\varphi}+i\sqrt{k^2\gamma^2+\hat{w}_m^2\sin^2\varphi}\right]}, \tag{57}$$

where $\hat{w}_m = -\sqrt{k^2 - v_m^2}$, $\hat{v}_m = (k/\beta) - (2\pi/a)m$, and r and φ are the polar coordinates in the xy plane (φ is measured from the negative y axis). The expressions of (57) were derived under the assumption that the charge is moving in the yz plane at a distance b from the edge of the structure. As we see from (57), the radiation field in free space is formed by superposition of conical waves diverging from the z axis. Here the wave vector of the m-th space harmonic makes an angle of

$$\theta_m = \arccos\left(\frac{1}{\beta} - \frac{2\pi m}{a}\right).$$

with the z axis. As in the case of a line source, the relation between the emission frequency and the observation angle θ_m is determined by the Doppler formula (2) for any value of the angle φ. The radiation field is symmetrical with respect to the yz plane. In this plane ($\varphi = 0$), apart from a constant factor, the expressions of (57) go over into the corresponding field formulas in the planar problem (the $E_{x\omega}$ component hereby vanishing).

The energy losses by emission into the free half-space can be determined from the energy flux through the surface of a circular cylinder of large radius described about the z axis. The spectral density of the emission losses per period of the structure in the angular interval from φ to $\varphi + d\varphi$ proves to be

$$W_\omega(\theta, \varphi) = \frac{e^2 ak}{4\pi c}\sum_m e^{-2b\sqrt{k^2\gamma^2+\hat{w}_m^2\sin^2\varphi}}$$

$$\times\frac{\frac{\hat{w}_m^2}{\beta^2}\sin^2\varphi + (k^2\gamma^2+\hat{w}_m^2\sin^2\varphi)\frac{\sqrt{k^2\cos^2\varphi+\hat{v}_m^2\sin^2\varphi}+\hat{w}_m\cos\varphi}{\sqrt{k^2\cos^2\varphi+\hat{v}_m^2\sin^2\varphi}-\hat{w}_m\cos\varphi}}{\left|L_1\left(i\sqrt{k^2\gamma^2+\hat{w}_m^2\sin^2\varphi}\right)\right|^2\left|L_2(\hat{w}_m\cos\varphi)\right|^2(k^2\cos^2\varphi+\hat{v}_m^2\sin^2\varphi)}, \tag{58}$$

where the summation extends only over the emitted harmonics. To illustrate the directional properties of the emission, we show the graph (Fig. 13) of the angular distribution of emission in the first space harmonic for various particle velocities (β = 0.15, 0.4, 0.6, and 0.8). Figures 13a–d show the curves of the emission intensity as a function of the angle θ($W_\omega = W_\omega(\theta)$) in planes corresponding to fixed values of the angle φ. One can readily visualize the three-dimensional emission distribution surfaces. We see that intense emission occurs in a narrow sector of angles near the normal to the particle trajectory. At low velocities ($\beta \leq 0.5$), the emission in the transverse direction can exceed by a factor of several-fold the maximum emission in the direction of motion. At relativistic velocities the forward emission is largely cut off, while the emission in the transverse direction remains very intense. Equation (58) is simplified considerably for two principal planes: $\varphi = 0°$ and

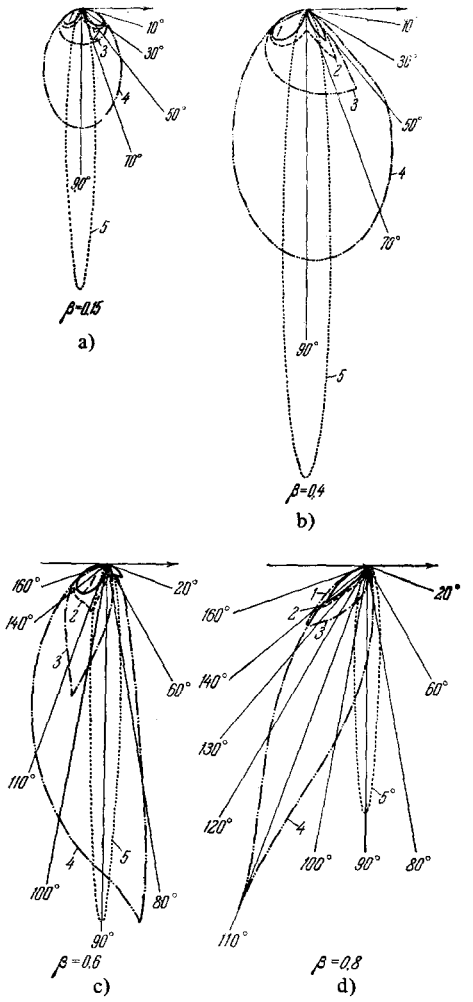

FIG. 13.

1 — φ = 0°; 2 — φ = 10°; 3 — φ = 20°; 4 — φ = 40°; 5 — φ = 85°.

$\theta_m = 90°$. In the plane passing through the trajectory of the charge and normal to the edges of the plates ($\varphi = 0°$), the directional diagram of the emission differs from the corresponding angular distribution in the two-dimensional case only in the factor $\sin\theta$. In the plane normal to the trajectory of the source ($\theta = 90°$), a harmonic of number m is emitted only at the frequency $\omega = 2\pi mu/a$, which is a multiple of the frequency of passage of the source through a period of the structure. The angular distribution of the emission in this plane for various source velocities is shown in Fig. 14.

3. Emission from a Line Source Passing Close to a Comb-like Structure

In deriving an exact solution in the last section, we adopted as the periodic structure a highly idealized model consisting of a set of half-planes. It is of more practical interest to treat comb-like retarding structures in which the dimensions (the depth) of the resonator regions are finite. Studying such structures makes it possible to elucidate the relation of the emission intensity to the depth of the cells. This proves to be a resonance relationship in a number of cases.

Figure 15a shows a two-dimensional comb-like retarding structure. It consists of infinitely long (along the

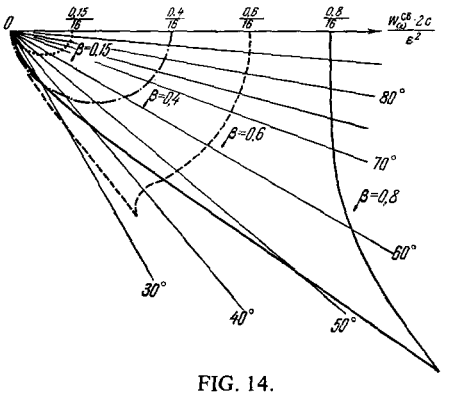

FIG. 14.

x axis), parallel, thin, ideally-conductive strips of width l. The strips are attached to a metallic plane (y = 0), or base, and are separated by the distance a. Let us take as the source of the field a uniformly-charged filament parallel to the x axis and moving at the constant velocity u at the "impact parameter" b from the edge of the structure.

It is convenient to use the image method in formulating the problem. The sought field of the moving filament evidently coincides for $y \leq 0$ with the field of the source plus its image relative to the plane y = 0 (a filament of linear charge density $-\epsilon$ situated at $y = b + l$) moving close to a periodic array of parallel, ideally-conductive strips of width $2l$ (Fig. 15b). We can formulate the problem as a system of integral equations for the unknown current distributions induced by the source in the plates of the structure. The method of deriving these equations has been discussed in detail in the review[2], and we shall give the equations here without deriving them:

$$\int_{-\infty}^{\infty} F(w)\,L(w)\cos wy\,dw = -\frac{\varepsilon\omega}{\pi i u}\,e^{-(l+b)k\gamma}\,\mathrm{ch}\,k\gamma y \quad \text{when } |y|<l,$$

$$\int_{-\infty}^{\infty} F(w)\cos wy\,dw = 0 \quad \text{when } |y|>l. \tag{59}$$

Here F(w) is the Fourier amplitude of the current-density distribution on the plate of number m = 0:

$$j_{0y}(y) = \int_{-\infty}^{\infty} F(w)\cos wy\,dw. \tag{60}$$

The representation (60) reflects the fact that the distri-

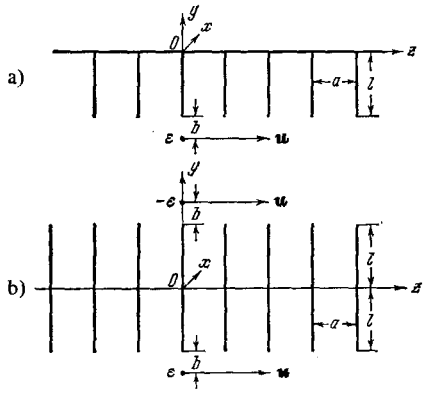

FIG. 15.

bution of the induced current and its image with respect to the base plane (on a strip of width $2l$) is an even function. The induced current $j_{0y}(y)$ determines the radiation field. The overall field equals the sum of the radiation field and the field of the source and its image moving in free space. The kernel L(w) is defined by Eq. (6, 10) of the review[2]:

$$L(w)=\frac{v\sin va}{\cos av-\cos a\frac{\omega}{u}}. \tag{61}$$

The system of equations (59) can be solved by the factoring method.[18] It is found in the form

$$F(w)=\frac{e^{iwl}}{(\kappa-w)L_2(w)}\left(K+\sum_{t=0}^{\infty}K_t\frac{w-w_t}{w+w_t}\right)+\frac{e^{-iwl}}{(k+w)L_1(w)}\left(K+\sum_{t=0}^{\infty}K_t\frac{w+w_t}{w-w_t}\right), \tag{62}$$

where w_t is determined by Eq. (50), and $L_1(w)$ and $L_2(w)$ by Eq. (51). The constant coefficients K and K_t must be defined such that the equations (59) are satisfied.

The chosen form of solution for F(w) is equivalent to representing the current in the strips bounding a cell of the structure as a superposition of current waves (corresponding to the fields of the normal modes of the waveguide for this region). These waves run both toward the interior of the cell and toward its open end. As we can easily verify, when the series $\sum_t K_t$ converges, the solution (62) satisfies the known conditions at the edges of the plates ($y=\pm l$): $F(w)\sim w^{3/2}$ as $w\to\infty$. We also note that when $w\to 0$, the function F(w) defined by Eq. (62) behaves completely analogously to the solution of the problem of a system of half-infinite plates. This indicates an identical law of decline of the electromagnetic field with distance in the remote region in both problems.

Substituting Eq. (62) into the system of integral equations (59) gives a linear inhomogeneous system of algebraic equations for the coefficients K and K_t:

$$K_t=\Gamma_t\left(K+\sum_{m=0}^{\infty}K_m\frac{w_t-w_m}{w_t+w_m}\right)\qquad(t=0,\ 1,\ 2,\ \ldots),$$

$$K+\sum_{m=0}^{\infty}K_m\frac{ik\gamma-w_m}{ik\gamma+w_m}=-\frac{\varepsilon\omega\gamma a}{4\pi^2iu\,(1+i\gamma)\,L_1(ik\gamma)}e^{-k\gamma b}. \tag{63}$$

Here we have introduced the quantity

$$\Gamma_t=\alpha_t\frac{\left[1+(-1)^t\cos\frac{ka}{\beta}\right](k+w_t)^2}{a^2w_t^2(w_t^2+k^2\gamma^2)}L_1^2(w_t)\,e^{2iw_tl},$$

where

$$\alpha_t=\begin{cases}\frac{1}{2}\text{ when }\ t=0,\\ 1\text{ when }\ t\geqslant 1.\end{cases} \tag{64}$$

We note that at any frequency the wave numbers w_t become purely imaginary above a certain value of the subscript t close to ka/π. Here the corresponding waveguide harmonics cease to propagate in the waveguide formed by two adjoining plates. For purely-imaginary values of w_t, the coefficients Γ_t contain the exponentially small factors ($\sim\exp\{-2\pi(e/a)t\}$ for large t). Hence we can approximately replace the infinite system (63) by a system having a finite number of unknowns by dropping the exponentially small coefficients K_t. Solving the abbreviated system gives approximate values of the coefficients K and K_t. Each time that we increase the number of unknowns by unity (i.e., take into account one of the damped waveguide harmonics in the resonator region), we increase the accuracy of the approximation.

Let us discuss several successive approximations. For very deep cells, in which the cell depth l is considerably greater than their period a, all the K_t coefficients are exponentially small. The approximate solution in this case has the form

$$K_t=0,$$

$$K=-\frac{\varepsilon\omega\gamma a e^{-k\gamma b}}{4\pi^2iu\,(1+i\gamma)\,L_1(ik\gamma)}\equiv B. \tag{65}$$

We can take this solution as the zero-order approximation. It coincides with the solution treated above in the problem of emission from a source moving near a system of half-infinite plates. We note that we have to assume that there is no wave reflected from the base in order to get the limiting transition $l\to\infty$. We can do this by assuming an infinitesimal attenuation.

In the frequency range

$$0\leqslant\frac{a}{\lambda}=\frac{ka}{2\pi}\leqslant\frac{1}{2} \tag{66}$$

only a TEM wave can propagate in the cell. For this wave, $w_0=k$ (the propagation constants of all the other waveguide harmonics are purely imaginary). Hence, in the first-order approximation, the infinite system (63) is reduced to two equations for the coefficients K and K_0:

$$K+K_0\frac{i\gamma-1}{i\gamma+1}=B,$$
$$K\Gamma_0-K=0. \tag{67}$$

Thus the solution in the first-order approximation has the form

$$K=-\frac{B}{\Delta_1},\quad K_0=\Gamma_0K, \tag{68}$$

where

$$\Delta_1=-\left(1+\Gamma_0\frac{i\gamma_0-1}{i\gamma_0+1}\right).$$

The second-order approximation for the frequency range of (66), i.e., the solution taking account of the exponentially-small K_1 and Γ_1, is defined by the expressions

$$\left.\begin{aligned}K&=\frac{B}{\Delta_2}\left[1+\Gamma_1\Gamma_0\left(\frac{k-w_1}{k+w_1}\right)^2\right],\\ K_0&=\frac{B}{\Delta_2}\Gamma_0\left[1-\Gamma_1\frac{w_1-k}{w_1+k}\right],\\ K_1&=\frac{B}{\Delta_2}\Gamma_1\left[1-\Gamma_0\frac{k-w_1}{k+w_1}\right],\end{aligned}\right\} \tag{69}$$

where

$$\Delta_2=1+\Gamma_0\frac{i\gamma-1}{i\gamma+1}+\Gamma_1\frac{ik\gamma-w_1}{ik\gamma+w_1}+\Gamma_0\Gamma_1\frac{k-w_1}{k+w_1}\left(\frac{k-w_1}{k+w_1}-\frac{ik\gamma-w_1}{ik\gamma+w_1}+\frac{i\gamma-1}{i\gamma+1}\right).$$

For numerical calculations, it is convenient to use an explicit expression for the coefficients Γ_t in the form of an infinite product:

$$\Gamma_t=e^{2iw_t\frac{a}{\pi}\left(\pi\frac{l}{a}-\ln 2\right)}\prod_{\substack{m=0\\ m\neq t}}^{\infty}\frac{w_m+w_t}{w_m-w_t}\prod_{m=1}^{\infty}\frac{(\hat{w}_{-m}-w_t)}{(\hat{w}_{-m}+w_t)}\frac{(\hat{w}_{+m}-w_t)}{(\hat{w}_{+m}+w_t)}. \tag{70}$$

As the representation (70) implies, the cited approximations converge only under the condition

$$r=\frac{l}{a}>\frac{\ln 2}{\pi}\approx 0.22, \tag{71}$$

i.e., for sufficiently closely-spaced or deep structures.

When the condition (71) is violated, the choice of a solution in the form of a superposition of waveguide harmonics is evidently inappropriate.

In treating emission at higher frequencies, we must take a system of higher order as the first-order approximation. Thus, we should naturally begin to find an approximate solution in the frequency range

$$\frac{s-1}{2} \leqslant q = \frac{ka}{2\pi} \leqslant \frac{s}{2}$$

with a system of order s + 1, since the coefficients K_t become exponentially small only when t > s + 1.

Determining the coefficients K and K_t solves the problem of finding the spectral component F(w) of the current in (62). Using F(w), we can easily write down the only non-zero component $H_{\omega x}$ of the magnetic field:

$$H_{\omega x}(y,\ z) = H_x^0 + \frac{2\pi}{c} e^{i\frac{k}{\beta}an} \int_{-\infty}^{\infty} F(w) \frac{\cos v\,[z-a(n+1)] - e^{i\frac{k}{\beta}a} \cos v\,(z-an)}{\cos av - \cos\frac{ak}{\beta}} \cos wy\, dw$$
$$(an \leqslant z \leqslant a(n+1)), \qquad (72)$$

where $H^0_{\omega x}$ is the field of the charged filament and its image in the metallic plane y = 0. The integration is performed by means of residues. The physical features of the field depend on whether it is calculated in a resonator cell ($-l < y < 0$) or in free space ($y < -l$). In a cell of the structure, the overall field is a superposition of standing waves made of waveguide harmonics propagated into the cell and reflected from the base:

$$H_{\omega x}(y,\ z) = -\frac{16\pi^2 i}{c} e^{i\frac{k}{\beta}an} \sum_{m=0}^{a} K_m \frac{(-1)^{mn} e^{i\omega m l} \cos w_m y \cos\frac{m\pi}{a} z}{(k+w_m) L_1(w_m) [1-(-1)^m e^{-i\frac{k}{\beta}a}]}$$
$$(-l \leqslant y \leqslant 0). \qquad (73)$$

The magnetic field of the charged filament excited in the free half-space has the form

$$H_{\omega x}(y,\ z) = -\frac{\varepsilon}{c} \operatorname{sgn}(y+b+l)\, e^{-k\gamma|y+b+l| + i\frac{k}{\beta}z}$$
$$+ \frac{2\pi^2}{ac} \sum_{t=0}^{\infty} \frac{\hat{v}_t}{\hat{w}_t (k+\hat{w}_t) L_1(\hat{w}_t)} \left(K + \sum_{m=0}^{\infty} K_m \frac{\hat{w}_t + w_m}{\hat{w}_t - w_m}\right) e^{i\hat{w}_t(y+l) + i\hat{v}_t z} \quad (y < -l),$$
$$\hat{v}_t = \frac{k}{\beta} - \frac{2\pi}{a} t. \qquad (74)$$

Here the first term defines the intrinsic field of the moving charged filament. The second term in (74) describes a superposition of plane electromagnetic waves excited by the source. The term of the summation corresponding to the subscript t = 0 gives a surface wave propagated along the structure synchronously with the source. The rest of the terms in the summation are space harmonics of the same frequency as the surface wave. Real values of the wave numbers $\hat{w}_t$ correspond to electromagnetic waves emitted by the moving source. Imaginary values of $\hat{w}_t$ correspond to inhomogeneous plane waves running over the structure at a velocity

$$u_t = u\left(1 - \frac{\lambda}{a}\frac{u}{c} t\right),$$

differing from the velocity of the source.

Now we shall discuss the energy characteristics of the emission that appears when the charged filament moves near the comb-like structure. We can determine the overall energy losses of the moving source by calculating the radiation reaction, i.e., the work done by the excited field on the source. When the source passes over one period of the structure ($0 \leq z \leq a$), the emission losses have the form

$$W = -\int_0^a dz \cdot 2\,\mathrm{Re} \int_0^{\infty} \varepsilon E_{z\omega}(z = ut,\ y = -l-b)\, e^{-i\omega t}\, d\omega = \int_0^{\infty} W_\omega\, d\omega. \qquad (75)$$

The spectral density of losses W_ω by emission is

$$W_\omega^{\mathrm{tot}} = -\frac{8\pi^2\varepsilon}{ku} e^{-k\gamma b} \mathrm{Re}\left\{\frac{1}{(1+i\gamma) L_1(ik\gamma)} \left(K + \sum_{t=0}^{\infty} K_t \frac{ik\gamma + w_t}{ik\gamma - w_t}\right)\right\}. \qquad (76)$$

We should note that only a retarded space harmonic moving synchronously with the source contributes to the expression for the radiation reaction at the frequency ω. The phase of the field of the rest of the space harmonics at the same frequency at the site of the source varies periodically because of the velocity difference between these harmonics and the charged filament. Hence, the work done by the field of these space harmonics on the source is zero when averaged over a period.

The expression for the emission losses from the moving source can also be derived directly by calculating the energy flux through a plane parallel to x and z, remote from the comb structure. The flux of the Poynting vector through a strip of width a in this plane determines the sought spectral density of emission losses per period of the structure:

$$W_\omega^{\mathrm{rad}} = -c \int_{an}^{a(n+1)} E_{\omega z} H_{-\omega x}\, dz$$
$$= \frac{16\pi^4}{a\omega} \sum_t \frac{\hat{v}_t^2}{\hat{w}_t (k+\hat{w}_t)^2} \left|\frac{1}{L_1(\hat{w}_t)} \left(K + \sum_{m=0}^{\infty} K_m \frac{\hat{w}_t + w_m}{\hat{w}_t - w_m}\right)\right|^2, \qquad (77)$$

where the summation over t covers all the space harmonics that can be emitted ($\hat{w}_t$ being real at the frequency in question).

We can determine approximate values of the coefficients K and K_t by Eqs. (68) or (69). Then we can use them in Eqs. (76) and (77) to calculate the emission losses at the different desired degrees of accuracy. The amount of emission losses depends on the emission frequency ω, the period of the structure a, the depth of the cell l, the velocity of motion of the source u, and the impact parameter b. For convenience we can introduce three dimensionless parameters:

$$q = \frac{ka}{2\pi}, \quad r = \frac{l}{a}, \quad \beta = \frac{u}{c}. \qquad (78)$$

For a fixed value of the impact parameter b, the size of the losses depends only on these three parameters. We shall give below the results of numerical calculations for the case b = 0. In the calculations, we have fixed two of the three quantities of (78), and have studied the dependence of W on the third variable. Figure 16 shows the overall emission losses $W_\omega^{\mathrm{overall}}$ as a function of the dimensionless cell depth r for various fixed values of the parameters q and β. We see that the relation of W_ω^{tot} to r is nearly periodic. The graphs show for comparison the results obtained in the first-, second-, and third-order approximations. All the graphs of Fig. 16 are drawn for the value $\beta = 0.9$ (relativistic motion of the source) and q values of 0.80, 0.60, and 0.48. The sharp resonance relation to r calls for attention. Thus, at q = 0.80, the emission losses at resonance (r = 1.85)

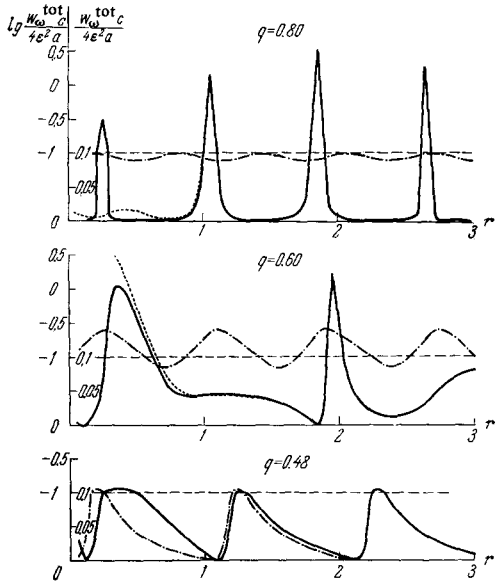

FIG. 16. $\beta = 0.9$.

exceed the losses at the same frequency for an infinitely deep structure by a factor of thirty.* We see that the first-order approximation is inapplicable for $q > 0.5$, while for $q < 0.5$ the results in the first- and second-order approximations agree satisfactorily. In the treated cases, the second- and third-order approximations give similar results. The agreement between the different orders of approximation improves with increasing r. We should note that at small r ($r < 0.22$) the method of calculation used here is inapplicable. Figure 17 shows for comparison the analogous $W_\omega(r)$ relations for $\beta = 0.4$ (non-relativistic motion of the source) and q values of 0.570 and 0.480.

We shall now proceed to discuss the spectral composition of the losses, i.e., the relation of W to q for fixed values of β and r. Figure 18 shows graphs of the $W_\omega(q)$ relation ($0 \leq q \leq 1$) for $\beta = 0.9$ for two values of the dimensionless cell depth r ($r = 1$ and $r = 5$). The result was obtained in the third-order approximation, which agrees very well with the second-order approximation. The graphs show a clearly marked resonance relation between the emission intensity and the frequency. The emission is concentrated in narrow resonance frequency bands where the intensity takes on high values. It is of interest to compare the curves of Fig. 18 with the spectral distribution of emission losses depicted in Fig. 9, when the source was passing close to the periodic structure made of half-planes ($r \to \infty$). We see that the emission for the structure with $r = 1$ at $\beta = 0.9$ at the frequency $q = 0.82$ exceeds that in the same spectral region for the infinitely deep structure by a factor of about twenty. As we increase the depth of the structure, the number of lines in the emission spectrum (i.e., the number of resonance maxima) increases, and the spectral lines become narrower. Figure 19 shows the corresponding spectral dependences of the intensity

*The size of the resonance maximum for $q = 0.874$ and $r = 1.6$ exceeds the losses for an infinitely deep structure under the same conditions by a factor of approximately 200 (!).

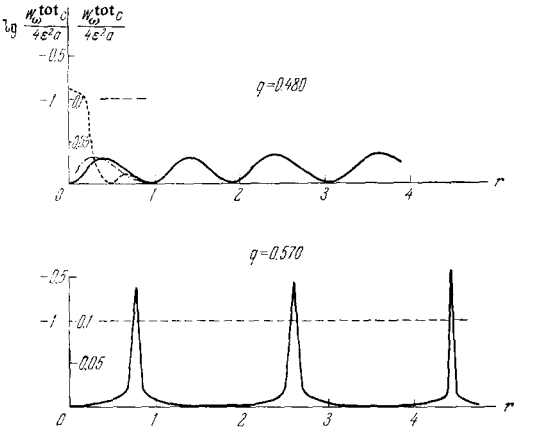

FIG. 17. $\beta = 0.4$.

for non-relativistic motion of the source ($\beta = 0.2$). The emission in this case is also of resonance type, although the maximum intensities are not so large.

Figures 20a and b aid in getting a picture of the relief of the function $W(q, \beta)$ in the $q\beta$ plane at the chosen depths r of the structure ($r = 1$ in Fig. 20a and $r = 5$ in Fig. 20b). These diagrams show the positions and heights of the resonance maxima. As the cited numerical values indicate, the relief of the $W(q, \beta)$ function is reminiscent of mountain ranges almost parallel to the β axis. The solid lines drawn on the graph show how the peaks of these mountain ranges are arranged. The dashed lines indicate the boundaries of the regions of emission of the space harmonics, as determined by the inequalities (15). A more detailed analysis of the quantitative results and also a number of graphic qualitative explanations of the characteristics of the diffraction emission in this case can be found in [25]. We also note that one can derive in a quite analogous way a solution of the problem of emission from sources passing near a transparent grating made of thin strips of finite height, as shown in Fig. 15b. In the latter case, one has to solve the problem of finding both the even and odd current distributions in the plates of the periodic structure.

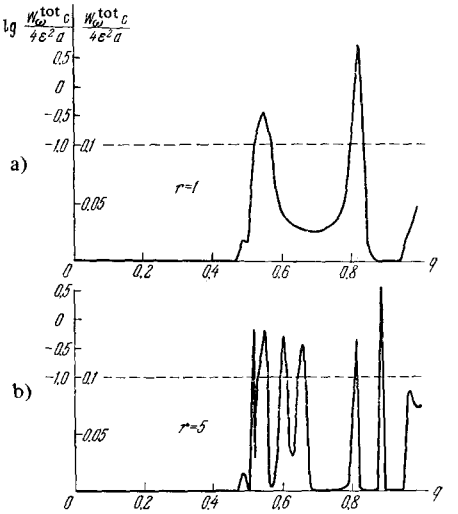

FIG. 18. $\beta = 0.9$.

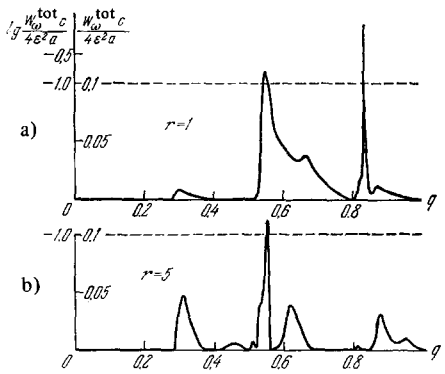

FIG. 19. $\beta = 0.2$.

4. OTHER METHODS OF CALCULATING THE EMISSION FROM SOURCES MOVING CLOSE TO PERIODIC STRUCTURES

Use of the factoring method discussed above leads to a solution in the form of successive approximations that converge very rapidly to the exact solution. However, this method can be applied only to study periodic structures of the discussed type. The methods of analysis developed in[26-30] provide broader potentialities. In these studies the authors were able to find an exact solution of the problem of emission from a plane modulated electron beam in the vicinity of a plane diffraction grating made of thin strips. The relation between the strip width and the period of the structure was arbitrary. They also found the quantitative characteristics of the emission for a grating made of thick bars and for an open comb-like structure having teeth of finite thickness. Following[26,27], we shall discuss in more detail the derivation of the solution and quantitative results for the case of a plane diffraction grating made of thin strips (see Fig. 2). We shall take the field source to be a plane modulated electron beam parallel to the grating and passing at a distance b from it:

$$\rho(z, t) = \rho_0 \delta(y - b)\, e^{i\left(\frac{\omega}{u} z - \omega t\right)}. \tag{79}$$

The field corresponding to such a current distribution in free space has a single component of the magnetic vector:

$$H_x(y, z) = -2\rho_0 \pi\beta e^{-k\gamma|y-b|} \operatorname{sgn}(y - b)\, e^{i\left(\frac{\omega}{u} z - \omega t\right)}. \tag{80}$$

The rest of the components of the electromagnetic field can be easily derived from (80) by the Maxwell equations. The radiation field generated by interaction of the source with the diffraction grating can be represented as a superposition of space harmonics:

$$H_x(y, z) = \operatorname{sgn} y \sum_{n=-\infty}^{\infty} B_n e^{i\left(\frac{\omega}{u} - 2\pi\frac{n}{d}\right) z + i\sqrt{k^2 - \left(\frac{\omega}{u} + \frac{2\pi n}{d}\right)^2}\,|y|}. \tag{81}$$

The coefficients B_n are proportional to the coefficients of the Fourier-series expansion of the current induced in the strips of the grating.

We can derive an equation for the coefficients B_n by requiring that the tangential component of the overall electric field should vanish at the plates of the grating (for $nd + a < z < (n + 1)d$), and that the tangential component of the magnetic field should vanish at the gaps in the grating (i.e., for $y = 0$, $nd < z < nd + a$). These two conditions give the following system of equations:

$$\sum_{n=-\infty}^{\infty} i\sqrt{k^2 - \left(\frac{\omega}{u} - \frac{2\pi n}{d}\right)^2}\, B_n e^{-i\frac{2\pi n}{d} z} = -2\pi\rho_0 e^{-k\gamma b}$$

for $nd + a < z < (n+1)d$ (at the strips of the grating),

$$\sum_{n=-\infty}^{\infty} B_n e^{-i\frac{2\pi n}{d} z} = 0 \quad \text{for} \quad nd < z < nd + a$$

(at the gaps of the grating). (82)

By making a formal substitution of variable $B_n = A_n/\hat{v}_n\rho_0$, we can[27] transform the system (82) into

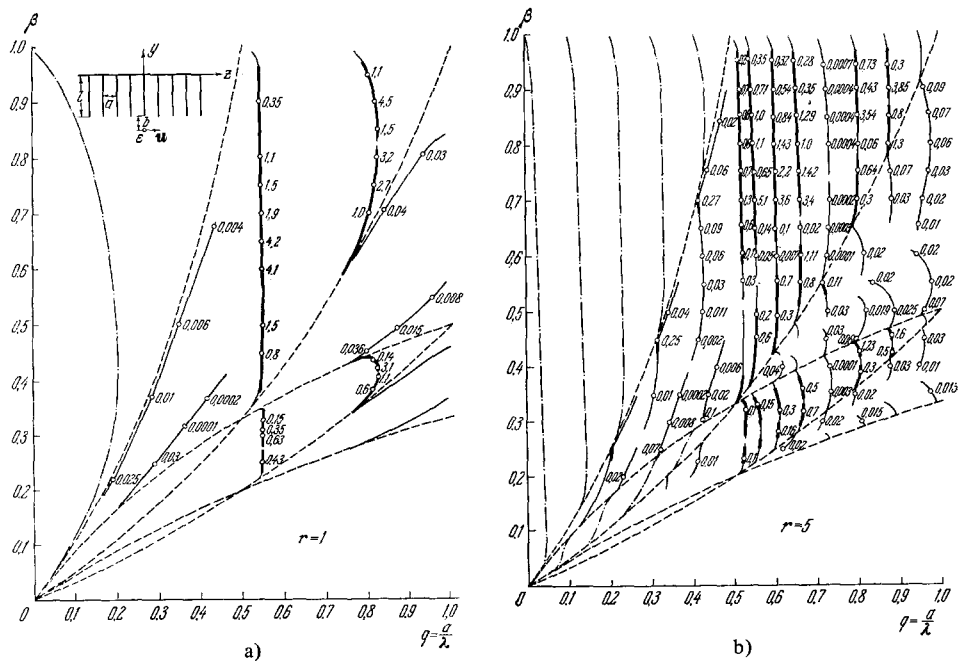

FIG. 20.

the form

$$\sum_{n=-\infty}^{\infty} A_n \frac{|n|}{n} e^{in\psi} = -\varepsilon + \sum_{n=-\infty}^{\infty} A_n \frac{|n|}{n} \chi_n e^{in\psi}, \quad 0 < \psi < \delta,$$

$$\sum_{n=-\infty}^{\infty} A_n e^{in\psi} = 0, \qquad \delta < \psi < 2\pi, \qquad (83)$$

where we have introduced the dimensionless variable $\psi = 2\pi z/d$ (correspondingly, $\delta = 2\pi a/d$). The quantities ϵ and χ_n are defined by the equations

$$\varepsilon = 2\pi e^{-k\gamma b},$$

$$\chi_n = 1 + i \frac{|n|}{n} \frac{|\hat{v}_n|}{\hat{v}_n} \sqrt{\frac{k^2}{\hat{v}_n^2} - 1}, \qquad (84)$$

while the quantity $\hat{v}_n$, which is the projection of the wave vector on the z axis, is defined by Eq. (50a). It is important to note for later reference that the quantity χ_n approaches zero ($\sim 1/n^2$) with increasing $|n|$.

Let us note here briefly the way to solve the system (83). Those interested in the details will find them in [26], which we are following in our treatment. If the right-hand side of the first of the equations (83) contained an assigned function of ψ, then the system (83) would be equivalent to the Riemann-Hilbert problem, in which an analytic function is determined by conditions assigned at the boundary of a certain region. In fact, let us consider the auxiliary system of equations

$$\sum_n A_n e^{in\psi} \frac{|n|}{n} = f(e^{i\psi}), \qquad 0 < \psi < \delta,$$

$$\sum_n A_n e^{in\psi} = 0, \qquad \delta < \psi < 2\pi. \qquad (85)$$

We shall introduce a function of the complex variable z by defining its expansion in powers of $z = |z|e^{i\psi}$:

$$X(z) = \begin{cases} X^+(z) = \sum_{n \geq 0} A_n z^n, & |z| < 1, \\ X^-(z) = -\sum_{n<0} A_n z^n, & |z| > 1. \end{cases} \qquad (86)$$

Then the left-hand sides of the equations contained in the system (85) are respectively the sum and difference of the limiting values of the function X(z) inside and outside the unit circle:

$$\left.\begin{aligned} X^+(e^{i\psi}) + X^-(e^{i\psi}) &= f(e^{i\psi}), \quad 0 < \psi < \delta, \\ X^+(e^{i\psi}) - X^-(e^{i\psi}) &= 0, \qquad \delta < \psi < 2\pi. \end{aligned}\right\} \qquad (87)$$

The first condition indicates a discontinuity in the function X(z) in passing along the arc of the circle having $0 < \psi < \delta$. The second condition indicates that the function X(z) is continuous in z over the rest of the circle. The problem of determining the function X(z) according to these conditions is precisely the Riemann-Hilbert problem.

Let us make a cut in the plane of the complex variable z along the arc L_1 (Fig. 21). Then let us form the function $X(z)\sqrt{(z-\alpha)(z-\bar{\alpha})}$, where α and $\bar{\alpha}$ are the end points of the arc L_1 ($\bar{\alpha} = 1$, $\alpha = e^{i\delta}$). This function is holomorphic, single-valued, and bounded at infinity. Consequently, it can be represented as a Cauchy integral

$$X(z)\sqrt{(z-\alpha)(z-\bar{\alpha})} = \frac{1}{2\pi i} \int_\Gamma \frac{X(\zeta)\sqrt{(\zeta-\alpha)(\zeta-\bar{\alpha})}}{\zeta - z} d\zeta + C, \qquad (88)$$

where the contour Γ surrounds the cut L_1, and the constant C has been obtained by reference to an infinitely distant point.

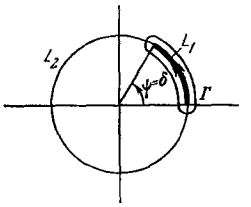

FIG. 21.

Now let us make the contour Γ approach the arc L_1. Taking into account the fact that the limiting values of the square root on the different sides of the cut differ in sign, while the limiting values of the function $X(\zeta)$ along the different sides of the cut are $X^+(z)$ and $X^-(z)$, we get

$$X(z)\sqrt{(z-\alpha)(z-\bar{\alpha})} = \frac{1}{2\pi i} \int_{L_1} \frac{X^+(\zeta) + X^-(\zeta)}{\zeta - z} \sqrt{(\zeta-\alpha)(\zeta-\bar{\alpha})}\, d\zeta + C. \qquad (89)$$

Upon substituting the values of $X^+(\zeta) + X^-(\zeta)$ from (87) into this formula, we obtain the solution of the Riemann-Hilbert problem.

Equation (89) permits one to find a relation between the values of X(z) on the circle of unit radius. If the point z approaches the arc L_1, the limiting value of the integral in (89) is determined by the formula of Sokhotskiĭ [31], and it depends on whether the point z approaches the arc from inside or outside the circle. Taking the average of these two limiting values, we get

$$\sum A_n e^{in\psi} = \sum A_n \zeta_0^n = X^+(\zeta_0) - X^-(\zeta_0)$$

$$= \frac{R(\zeta_0)}{\pi i} \int_{L_1} \frac{f(\zeta_0)}{\zeta - \zeta_0} \sqrt{(\zeta-\alpha)(\zeta-\bar{\alpha})}\, d\zeta + 2CR(\zeta_0), \qquad (90)$$

where

$$R(\zeta) = \begin{cases} \frac{1}{\sqrt{(\zeta-\alpha)(\zeta-\bar{\alpha})}} & \text{on the arc } L_1, \\ 0 & \text{on the arc } L_2, \end{cases}$$

and the integral is understood to have its principal value. The point ζ_0 is taken on the circle of unit radius. Equation (90) implies that A_n is the coefficient in the Fourier-series expansion of the right-hand side.

Now let

$$f(\zeta_0) = -\varepsilon - \sum_{n=-\infty}^{\infty} A_n \frac{|n|}{n} \chi_n e^{in\psi},$$

as is the case in the real system of equations (83). Substitution of this expression into (90) and calculation of the Fourier coefficients for both sides of the equation leads to an infinite system of algebraic equations for the coefficients A_n. This system of equations can be solved to the required accuracy, since it contains the small parameter χ_n (we recall that the definition (84) implies that χ_n becomes small for large n). Adopting a given degree of accuracy of solving the infinite system of equations for the coefficients A_n, we can replace the system with a finite number of equations. The required number n of equations is equal in order of magnitude to the ratio of the period a of the structure to the wavelength λ (more exactly, $n > a/\lambda\beta$). Since there are standard programs for solving systems of linear algebraic equations, it is convenient to use computers to find the numerical values of the coefficients A_n.

We can determine the amount of emission losses per

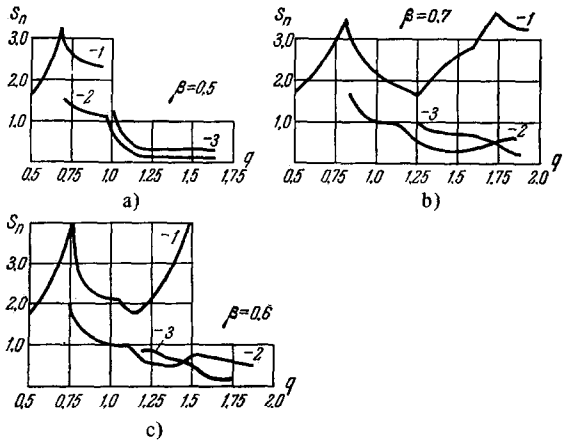

FIG. 22.

period of the structure by calculating the flux of the Poynting vector across a plane y = const. Here we have to bear in mind that the emission is distributed symmetrically with respect to the plane of the diffraction grating. The intensity S_n of the losses in the space harmonic of order n is proportional to $|A_n|^2$. The relation between the frequency and the propagation direction of the emitted wave is given by the Doppler relations (2) and (11), which are general for all linear periodic systems.

Graphs are given in [27] of the relation between the size of the Poynting vector S_n corresponding to different space harmonics and the parameters of the problem (the beam velocity β, the dimensionless grating period d/λ, and the filling coefficient a/d of the grating). They were obtained on a computer by the method described above. Figure 22, which is taken from [19], shows the relation of S_n (for $n = -1, -2, -3$) to the variable $q = l/\lambda$ for various velocities of the electron current (β = 0.5, 0.6, and 0.7). The grating filling coefficient is a/d = 0.5, i.e., the width of the strips in the grating was equal to the spaces between the strips. We see from the graphs that the emission intensity shows a resonance relation to q. For the chosen range of variation of the parameters, the most intense emission occurs in the first space harmonic. The relation of S_n to the grating filling coefficient for a given source velocity and fixed frequency is of interest. Figure 23 gives examples of such relations for the first space harmonic. As is quite evident, there is no emission in the limiting cases a/d = 0 and a/d = 1. There are maxima of emission at certain intermediate values of a/d.

The above-discussed method of finding the fields, which is based on solving the boundary Riemann-Hilbert problem, is applicable only to studying plane gratings made of infinitesimally thin strips. Structures consisting of bulk elements are of greater practical interest, e.g., diffraction gratings consisting of thick bars of comb-like structures having teeth of finite thickness (see Figs. 24 and 6). V. P. Shestopalov, O. A. Tret'yakov, and É. I. Chernyakov [28,29] have made a study of emission from charged sources moving past such structures, based on numerical methods. Here they reduced the diffraction-emission problem to a finite system of linear algebraic equations for the Fourier coefficients, the field being represented as a superposition of space harmonics analogous to the systems of (82). In [28,29] they developed procedures for effective quantitative study of the obtained infinite algebraic systems using computers. A rather detailed presentation of the method of calculation and also of the mathematical study of the obtained solutions whenever possible is given in [40]. We note that problems of excitation by a moving source of the cited periodic structures can easily be interrelated by the image method: the emission from a charge above a comb-like structure (of depth l, see Fig. 6) is equivalent to that excited by the symmetrical passage of two charges of opposite sign past both sides of a structure made of bars (of thickness $2l$). In comparison with a plane strip grating, a structure of the type shown in Figs. 6 and 24 is characterized by an additional parameter, the depth (or thickness) l of the elements of the structure. Hence it is of interest to study the relation of the emission characteristics to this parameter. Figure 25 shows the relation, as taken from [28], of the size of the Poynting vector S in the $n = -1$ harmonic to the source velocity for three different values of the thickness of the grating. For comparison, the dot-dash line gives the value of the Poynting vector for a plane strip grating. We note here that for a thick grating the emission is no longer symmetric with respect to the plane of symmetry of the grating, y = 0. The graph gives the values of the energy flux into the half-space ($y > l/2$) containing the source. Figure 26

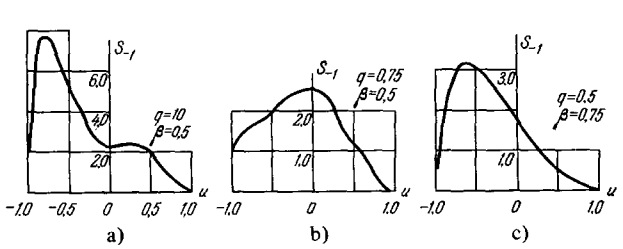

FIG. 23. $u = \cos(\pi a/d)$.

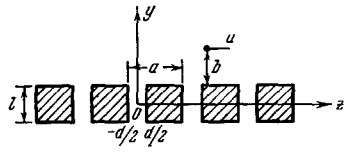

FIG. 24

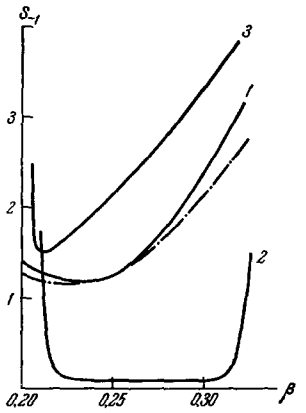

FIG. 25. $d/a = 0.2$, $q = 0.25$.
1 — $l/a = 0$; 2 — $l/a = 0.9$; 3 — $l/a = 1.8$.

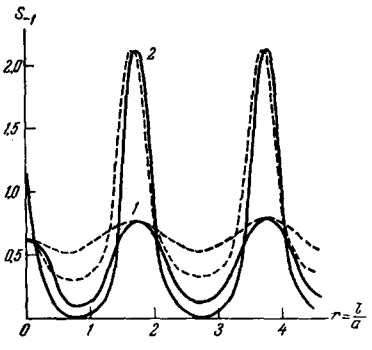

FIG. 26. $a/\lambda = 0.25$, $\beta = 0.249$.
1 — $d/a = 0.5$; 2 — $d/a = 0.2$.

shows the Poynting vector S_{-1} as a function of the grating thickness l. The solid lines show the characteristics of the emission above the grating, and the dotted lines give the emission below the grating ($y < -l/2$). The resonance nature of the variation is clearly visible.

There is a large number of graphs in [28,29] permitting one to get an idea of some of the features of the emission. However, the values of the parameters chosen for calculation apply only to the case of emission along the normal to the plane of the grating. Thus the contribution to the emission from currents parallel to the y axis (see Fig. 24) is not taken into account. At the same time, as was shown in Sec. 3, such currents can give rise to strong resonance peaks of emission intensity at angles differing from the normal to the structure.

In addition to the rigorous methods of study based on numerical analysis of the derived equations with computers, as developed in [28,29], one can find an approximate analytic solution in dealing with gratings in which the slit width is considerably smaller than the period. It describes the characteristic features of the emission rather fully. This approximate approach is based on formulating the problem in the form of infinite systems of linear algebraic equations of the second kind. For example, an analysis of a derived approximate solution is found in [41].

One can find a number of generalizations of the problems discussed in this section in the collected volume [30].

CONCLUSION

We have discussed above the diffraction emission that arises when charged sources move alongside open periodic structures. The discussed problems greatly resemble problems of emission from charged particles in layered periodic media. In particular, the emission spectrum is described by analogous Doppler relations. The essential difference between the cited problems is the fact that, in studying diffraction emission, the source moves in a vacuum, while in the latter case optical inhomogeneities along the trajectory of the source are directly due to the periodic variation of the properties of the medium in which the source is moving. This physical distinction gives rise to a difference in the methods of mathematical analysis of the problem. We are not discussing emission in layered periodic media, but shall cite only the references to the fundamental studies [32-36] on this problem and the review [37].

Above, we have treated the emission in an approximation involving uniform motion of the source: the reverse effect of the emission on the source has not been taken into account. However, if the path of the charge near the grating is long enough, and the emitting charges or currents are large enough, it becomes unjustified to neglect the radiation reaction. The radiation reaction can cause an additional modulation of the original charge distribution in the beam, and thus considerably alter the characteristics of the emission. Preliminary results are given in [38] of calculations of the growth of space-charge waves in an initially homogeneous beam moving in the space between two plane diffraction gratings. The results obtained in [38] indicate the importance of studying self-consistent problems for each concrete case.

We should mention the interesting study undertaken by I. L. Verbitskiĭ of the induction of oscillations in an initially single-velocity plane electron beam moving above a comb-like structure in a waveguide.

Note added in proof. Since this review was submitted for publication, several studies have appeared, and should be mentioned at least briefly. In [42] emission was studied from a charged particle passing by an assemblage of ideally-conductive half-planes. The results match those of the studies cited above. In [41,43] emission was studied from a charged particle moving in the helical waveguide. In [44], the theory is discussed of the Wood anomalies, which were referred to on pp. 150-151 of this review.

[1] V. L. Ginzburg and I. M. Frank, Zh. Eksp. Teor. Fiz. 16, 15 (1946).

[2] B. M. Bolotovskiĭ and G. V. Voskresenskiĭ, Usp. Fiz. Nauk 88, 209 (1966) [Sov. Phys.-Usp. 9, 73 (1966)].

[3] B. M. Bolotovskiĭ, G. V. Voskresenskiĭ, V. I. Gaĭduk, N. A. Ovchinnikova, and A. M. Kharchenko, Proceedings of the 21st All-Union Scientific Session, Electronics Section, M., 1965, p. 12.

[4] I. M. Frank, Izv. AN SSSR, ser. fiz. 6, 3 (1942).

[5] S. J. Smith and E. M. Purcell, Phys. Rev. 92, 1069 (1953).

[6] Electronics, Oct. 19, 74 (1962).

[7] F. S. Rusin and G. D. Bogomolov, ZhETF Pis. Red. 4, 236 (1966) [JETP Lett. 4, 160 (1966)].

[8] L. D. Landau and E. M. Lifshitz, Teoriya polya (Field Theory), M., Fizmatgiz, 1960; Engl. Transl., The Classical Theory of Fields, Addison-Wesley, Reading, Mass., 1962.

[9] K. Ishiguro and T. Tako, Optica Acta 8, 25 (1961).

[10] A. J. Fox and N. W. W. Smith, Proc. IEEE 52, 429 (1955).

[11] B. Z. Katsenelenbaum, Zh. Tekh. Fiz. 25, 546 (1955).

[12] V. B. Braginskiĭ, Radiotekhnika i élektronika 1, 232 (1956).

[13] V. N. Parygin, Izv. Vuzov (Radiofizika) 1, 139 (1958).

[14] C. W. Barnes and K. G. Dedrick, J. Appl. Phys. 37, 411 (1966).

[15] B. M. Bolotovskiĭ and A. K. Burtsev, Optika i Spektroskopiya 19, 470 (1965) [Optics and Spectroscopy 19, 263 (1965)].

[16] G. Toraldo di Francia, Nuovo cimento 16, 61 (1960).

[17] A. Hessel, Can. J. Phys. 42, 1195 (1964).

[18] L. A. Vaĭnshteĭn, Teoriya difraktsii i metod faktorizatsii (Diffraction Theory and the Factoring Method), M., "Sov. radio", 1966.

[19] B. Noble, Methods Based on the Wiener-Hopf Technique for the Solution of Partial Differential Equations, Pergamon Press, New York, 1958; Russ. Transl., M., IL, 1962.

[20] B. M. Bolotovskiĭ and G. V. Voskresenskiĭ, Zh. Tekh. Fiz. 34, 1856 (1964) [Sov. Phys. Tech. Phys. 9, 1432 (1965)].

[21] G. V. Voskresenskiĭ and B. M. Bolotovskiĭ, Dokl. Akad. Nauk SSSR 156, 770 (1964) [Sov. Phys. Dokl. 9, 459 (1964)].

[22] E. V. Avdeev and G. V. Voskresenskiĭ, Radiotekhnika i élektronika 11, 1560 (1966).

[23] E. V. Avdeev and G. V. Voskresenskiĭ, ibid. 11, 1419 (1966).

[24] E. V. Avdeev and G. V. Voskresenskiĭ, ibid. 12, 469 (1967).

[25] E. V. Avdeev and G. V. Voskresenskiĭ, Izv. vuzov (Radiofizika) 11, No. 1 (1968).
[26] Z. S. Agranovich, V. A. Marchenko, and V. P. Shestopalov, Zh. Tekh. Fiz. 32, 381 (1962) [Sov. Phys. Tech. Phys. 7, 277 (1962)].
[27] O. A. Tret'yakov, S. S. Tret'yakova, and V. P. Shestopalov, Radiotekhnika i Élektronika 10, 10 (1965).
[28] O. A. Tret'yakov, É. I. Chernyakov, and V. P. Shestopalov, Zh. Tekh. Fiz. 36, 33 (1966) [Sov. Phys. Tech. Phys. 11, 22 (1966)].
[29] O. A. Tret'yakov, É. I. Chernyakov, and V. P. Shestopalov, Izv. vuzov (Radiofizika) 9, 342 (1966).
[30] Collected volume, Radiotekhnika (Radiotechnology), No. 1, Kh., Khar'kov State University Press, 1965.
[31] M. A. Lavrent'ev and B. V. Shabat, Metody teorii funktsiĭ kompleksnogo peremennogo (Methods of the Theory of Functions of a Complex Variable), M., Gostekhizdat, 1951; Germ. Transl., Methoden der komplexen Funktiontheorie, VEB Deutscher Verlag der Wissenschaften, Berlin, 1967.
[32] Ya. B. Faĭnberg and N. A. Khizhnyak, Zh. Eksp. Teor. Fiz. 32, 883 (1957) [Sov. Phys.-JETP 5, 720 (1957)].
[33] M. L. Ter-Mikaélyan, Dokl. Akad. Nauk SSSR 134, 318 (1960) [Sov. Phys. Doklady 5, 1015 (1961)].
[34] G. M. Garibyan, Zh. Eksp. Teor. Fiz. 35, 1435 (1958) [Sov. Phys.-JETP 8, 1003 (1959)].
[35] G. M. Garibyan and I. I. Gol'dman, DAN ArmSSR 31, 219 (1960).
[36] L. Ronchi and G. Toraldo di Francia, Alta Frequenza 32, 558 (1963).
[37] F. G. Bass and V. M. Yakobenko, Usp. Fiz. Nauk 86, 189 (1965) [Sov. Phys.-Usp. 8, 420 (1965)].
[38] I. Palocz and A. A. Oliner, A Self-Consistent Theory of Cerenkov and Smith-Purcell Radiation, Proc. Symposium on Quasi-Optics, Polytechnic Press, Brooklyn, N. Y., 1964, pp. 217–233.
[39] R. W. Wood, Phys. Rev. 48, 928 (1935).
[40] S. A. Masalov, Dissertation, Khar'kov, 1965.
[41] V. G. Sologub, Dissertation, IRÉ AN Ukr.SSR, Khar'kov, 1967.
[42] J. Sam, J. Math. Phys. 8, 1053 (1967).
[43] A. R. Neureuther and R. Mittra, Proc. IEEE 55, 2134 (1967).
[44] B. M. Bolotovskiĭ and A. N. Lebedev, Zh. Eksp. Teor. Fiz. 53, 1349 (1967) [Sov. Phys.-JETP 26, 784 (1968)].

Translated by M. V. King